Heavy mineral and geochemical signatures of porphyry copper mineralization: examples from the Casino porphyry Cu-Au-Mo deposit, Yukon

M.B. McClenaghan[1], M.W. McCurdy[1], R.G. Garrett[2], C.E. Beckett-Brown[3], M.I. Leybourne[4, 5], S.G. Casselman[6], and P. Pelchat[1]

McClenaghan, M.B., McCurdy, M.W., Garrett, R.G., Beckett-Brown, C.E., Leybourne, M.I., Casselman, S.G., and Pelchat, P., 2021. Heavy mineral and geochemical signatures of porphyry copper mineralization: examples from the Casino porphyry Cu-Au-Mo deposit, Yukon; in *Targeted Geoscience Initiative 5: contributions to the understanding and exploration of porphyry deposits, (ed.) A. Plouffe and E. Schetselaar; Geological Survey of Canada, Bulletin 616, p. 159–202. https://doi.org/10.4095/327987*

Abstract: We report results of a detailed indicator mineral and geochemical study of the Casino calc-alkaline porphyry Cu-Au-Mo deposit in the unglaciated terrain of west-central Yukon. It is one of the largest and highest-grade porphyry Cu-Au-Mo deposits in Canada and is hosted by Late Cretaceous quartz monzonite and associated breccias. At 22 sites, a large (10–14 kg) stream-sediment sample, streamwater and stream silt samples were collected to compare geochemical and heavy mineral signatures. The Casino deposit has an obvious indicator mineral signature in the less than 2 mm heavy (>3.2 specific gravity (SG)) and mid-density (2.8–3.2 SG) fractions of stream sediments that is detectable at least 14 km downstream and consists of, in order of effectiveness, gold>chalcopyrite>molybdenite>sphalerite >jarosite>goethite>pyrite. Similar indicator mineral patterns occur in creeks downstream of other local porphyry occurrences (i.e. Cockfield, Zappa). The geochemical signature of the deposit is best defined by Ag, As, Au, Bi, Cd, Cu, Fe, Mn, Mo, Pb, U, and Zn in the less than 0.177 mm fraction of stream sediment and Cd, Co, Cu, Mo, Pb, Re, and Zn in stream water. Governments and exploration companies will benefit from adding indicator mineral sampling to routine stream-sediment sampling protocols during geochemical surveys in which detailed follow up during the same season is impossible.

Résumé : Dans le présent article, nous rendons compte des résultats d'une étude détaillée de la géochimie et des minéraux indicateurs du gisement porphyrique calco-alcalin à Cu-Au-Mo de Casino, situé dans le terrain ayant échappé à l'englaciation du centre ouest du Yukon. Il s'agit de l'un des gisements porphyriques à Cu-Au-Mo des plus grands et des plus riches au Canada. Il est encaissé dans une monzonite quartzique du Crétacé tardif et les brèches associées. À 22 sites, nous avons prélevé un gros échantillon (de 10 à 14 kg) de sédiments de ruisseau ainsi que des échantillons d'eau et de silt de ruisseau pour comparer leurs signatures géochimiques et en minéraux lourds. Le gisement de Casino présente une signature manifeste en minéraux indicateurs dans les composantes lourde (densité >3,2) et de densité moyenne (densité de 2,8 à 3,2) de la fraction <2 mm des sédiments de ruisseau. Cette signature peut être relevée jusqu'à au moins 14 km en aval et se manifeste par les minéraux suivants, par ordre d'efficacité : or>chalcopyrite>molybdénite>sphalérite>jarosite>goethite>pyrite. Des configurations de minéraux indicateurs semblables se retrouvent dans des ruisseaux en aval d'autres indices locaux de minéralisations porphyriques (c.-à-d. Cockfield, Zappa). La signature géochimique du gisement est mieux définie par les éléments Ag, As, Au, Bi, Cd, Cu, Fe, Mn, Mo, Pb, U et Zn dans la fraction <0,177 mm des sédiments de ruisseau et par les éléments Cd, Co, Cu, Mo, Pb, Re et Zn dans l'eau de ruisseau. Les gouvernements et les sociétés d'exploration minérale gagneraient à ajouter l'échantillonnage des minéraux indicateurs à leurs protocoles d'échantillonnage régulier de sédiments de ruisseau lors des levés géochimiques qui ne permettent pas de faire des suivis détaillés au cours de la même saison.

[1]Geological Survey of Canada, 601 Booth Street, Ottawa, Ontario K1A 0E8
[2]Emeritus Scientist, Geological Survey of Canada, 601 Booth Street, Ottawa, Ontario K1A 0E8
[3]Harquail School of Earth Sciences, Laurentian University, 935 Ramsey Lake Road, Sudbury, Ontario P3E 2C6
[4]Department of Geological Sciences and Engineering, Queen's University, 36 Union Street, Kingston, Ontario K7L 3N6
[5]McDonald Institute, Canadian Particle Astrophysics Research Centre, Stirling Hall, Department of Physics, Engineering Physics & Astronomy, Queen's University, Kingston, Ontario K7L 3N6
[6]Yukon Geological Survey, 300 Main Street, Whitehorse, Yukon Y1A 2B5
*Corresponding author: M.B. McClenaghan (email: beth.mcclenaghan@canada.ca)

INTRODUCTION

The recovery of indicator minerals from surficial sediments is a well established exploration method for gold (e.g. Averill, 2001; McClenaghan and Cabri, 2011) and diamonds (e.g. McClenaghan and Kjarsgaard, 2007) in glaciated terrain. Recently, indicator mineral methods for porphyry copper exploration have been tested in glaciated (e.g. Kelley et al., 2011; Chapman et al., 2015, 2018; Hashmi et al., 2015; Canil et al., 2016; Plouffe et al., 2016; Pisiak et al., 2017; Plouffe and Ferbey, 2017, 2019) and unglaciated terrain (Averill, 2011). The objective of the Geological Survey of Canada's (GSC) Targeted Geoscience Initiative (TGI) porphyry indicator mineral research is to further develop a porphyry copper indicator mineral suite that can be used for surficial sediment sampling in both the glaciated and unglaciated regions of Canada (McClenaghan et al., 2018, 2019, 2020). This new research includes the detailed examination and chemical characterization of tourmaline (Beckett-Brown et al., 2019, this volume), magnetite (McClenaghan et al., 2019), epidote, rutile, and zircon (Kobylinksi et al., 2017, 2018; Plouffe et al., 2018, 2019, this volume).

One component of the TGI porphyry copper indicator mineral research is a study carried out at the Casino porphyry Cu-Au-Mo deposit (McClenaghan et al., 2018, 2019), one of Canada's largest and highest grade undeveloped porphyry Cu-Au-Mo deposits (Casselman and Brown, 2017). The Casino deposit was used as a test site because it has been minimally disturbed by exploration drilling, has not yet been mined, and is known to contain tourmaline, and because metal-rich sediments and waters are known to occur in local creeks draining the deposit (Archer and Main, 1971). Here we report the results of mineralogical and geochemical studies of the Casino deposit, including indicator minerals in stream sediments and the geochemistry of stream silt and water.

Location and access

The Casino study area is located in west-central Yukon, 300 km north of Whitehorse (Fig. 1), within the Klondike Plateau ecoregion (Smith et al., 2004) and NTS map areas 115J/10 and 115J/15. The deposit is at latitude 62°44′N and longitude 138°50′W, and is accessed by fixed-wing aircraft or helicopter. Creeks draining the northwest side of the deposit flow north and eventually drain into the Yukon River. Creeks draining the south side of the deposit eventually drain into the White River. Most of the terrain lies at elevations of 1000 to 1500 m a.s.l. The climate of the study area is cold and semiarid (Bond and Lipovsky, 2011) with a mean annual temperature of approximately –5.5°C (mean annual summer temperature: 10.5°C, mean annual winter temperature: –23°C), and the mean annual precipitation ranges from 300 to 450 mm (Smith et al., 2004).

GEOLOGY

Deposit discovery history

The earliest exploration in the Casino area was for placer gold in the lower reaches of Canadian Creek in 1911 (Bostock, 1959; Fig. 2). Further upstream on Canadian Creek, on the northwest flank of what is now the Casino deposit, a gold-tungsten placer occurrence was first worked to mine tungsten in 1916. When the upper gold-tungsten placer occurrence was worked again in 1940s, the following minerals were recovered from the black sand: ferberite, gold, magnetite, hematite, scheelite, molybdenite, zircon, cassiterite, tourmaline, and titanite (Bostock, 1959; Archer and Main, 1971). Over the years, placer gold mining also took place on Rude Creek (Fig. 2), 10 km southeast of the Casino deposit (Chapman et al., 2014). Other early exploration work in the Casino area focused on the silver-lead-zinc veins at the Bomber occurrence (Yukon Geological Survey, 2018a) on the southern periphery of what is now known as the Casino deposit (Fig. 2).

Prior to the initial diamond drilling that resulted in the discovery of Cu-Au-Mo mineralization, surface indications of the presence of the Casino deposit included the prominent (730 m long) limonite gossan along a small creek that drains into upper Casino Creek (Fig. 2) on the southeast side of the deposit; the presence of the local gold-tungsten placer occurrence; intense hydrothermal alteration; the presence of limonite, jarosite, and weak malachite staining in leached rocks at the surface; the peripheral silver-zinc-lead veins; and anomalous Cu concentrations in –80 mesh (<0.177 mm) stream silt samples in Casino Creek compared to values for the Dawson Range compiled over several years by Archer and Main (1971). Anomalous Cu and Mo in –80 mesh soil samples collected in 1968 were used to guide initial drilling in 1969 that revealed significant mineralization (Archer and Main, 1971). Current total measured, indicated, and inferred resources of the deposit are 101 000 000 t of 0.39 g/t Au in the oxide gold zone; 87 000 000 t grading 0.25% Cu, 0.29 g/t Au, 0.02% Mo, and 1.7 g/t Ag in the supergene oxide–enriched zone; and 2 700 000 000 t of sulfide ore grading 0.16% Cu, 0.19 g/t Au, 0.02% Mo, and 1.5 g/t Ag in the supergene sulfide and hypogene zones (Huss et al., 2013; Casselman and Brown, 2017).

Bedrock geology

The Casino deposit area is underlain by metamorphosed and deformed basement rocks of the Yukon-Tanana terrane, an allochthonous, tectonic terrane that extends more than 2000 km from Alaska, U.S.A., through Yukon, and south into British Columbia. The terrane consists of rocks formed in a mid- to late Paleozoic continental arc system that separated the Yukon-Tanana arc from the western margin of Laurentia (Nelson et al., 2006, 2013). The terrane consists

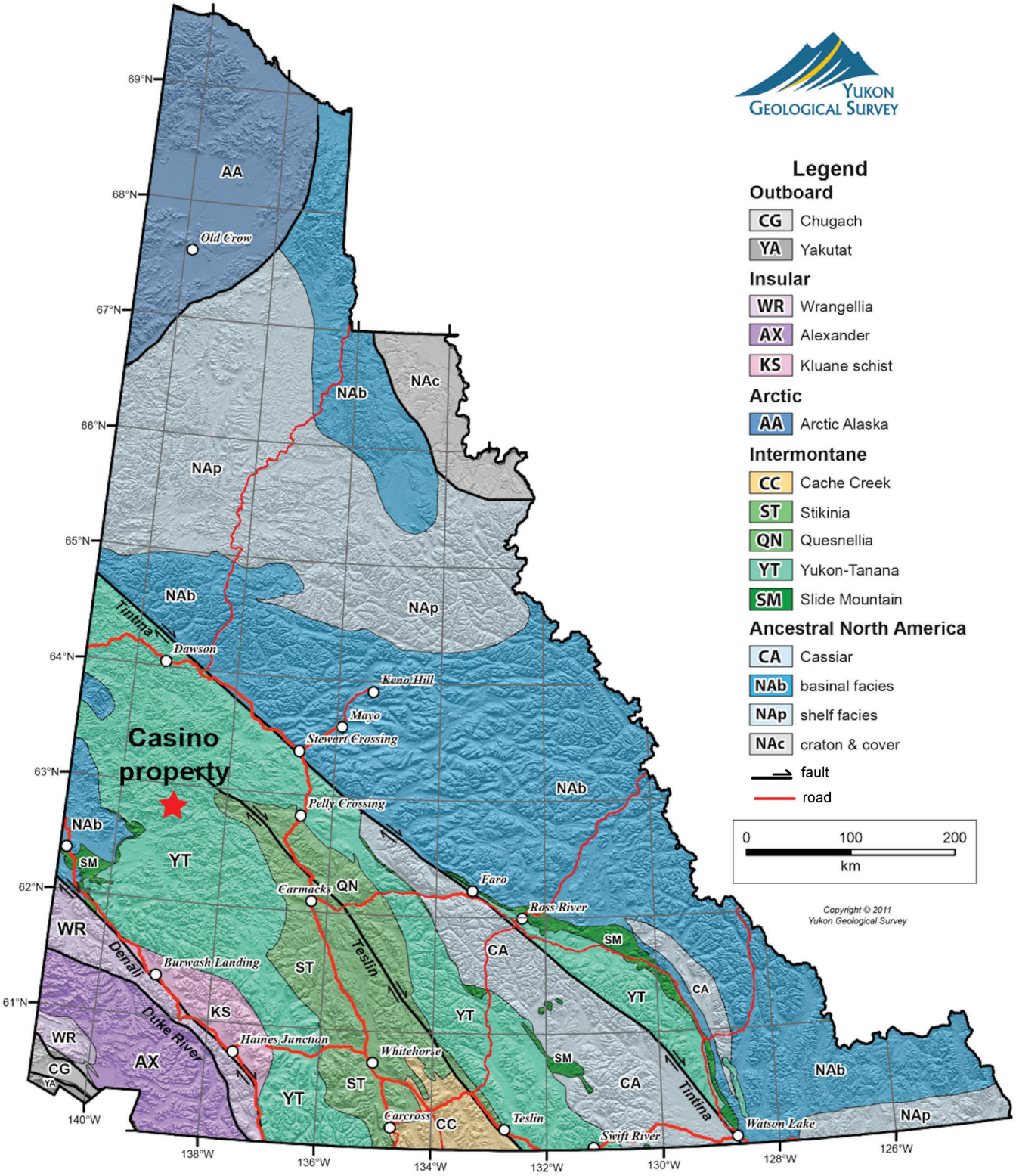

Figure 1. Location of the Casino porphyry copper deposit in west-central Yukon (*modified from* Relf et al., 2020).

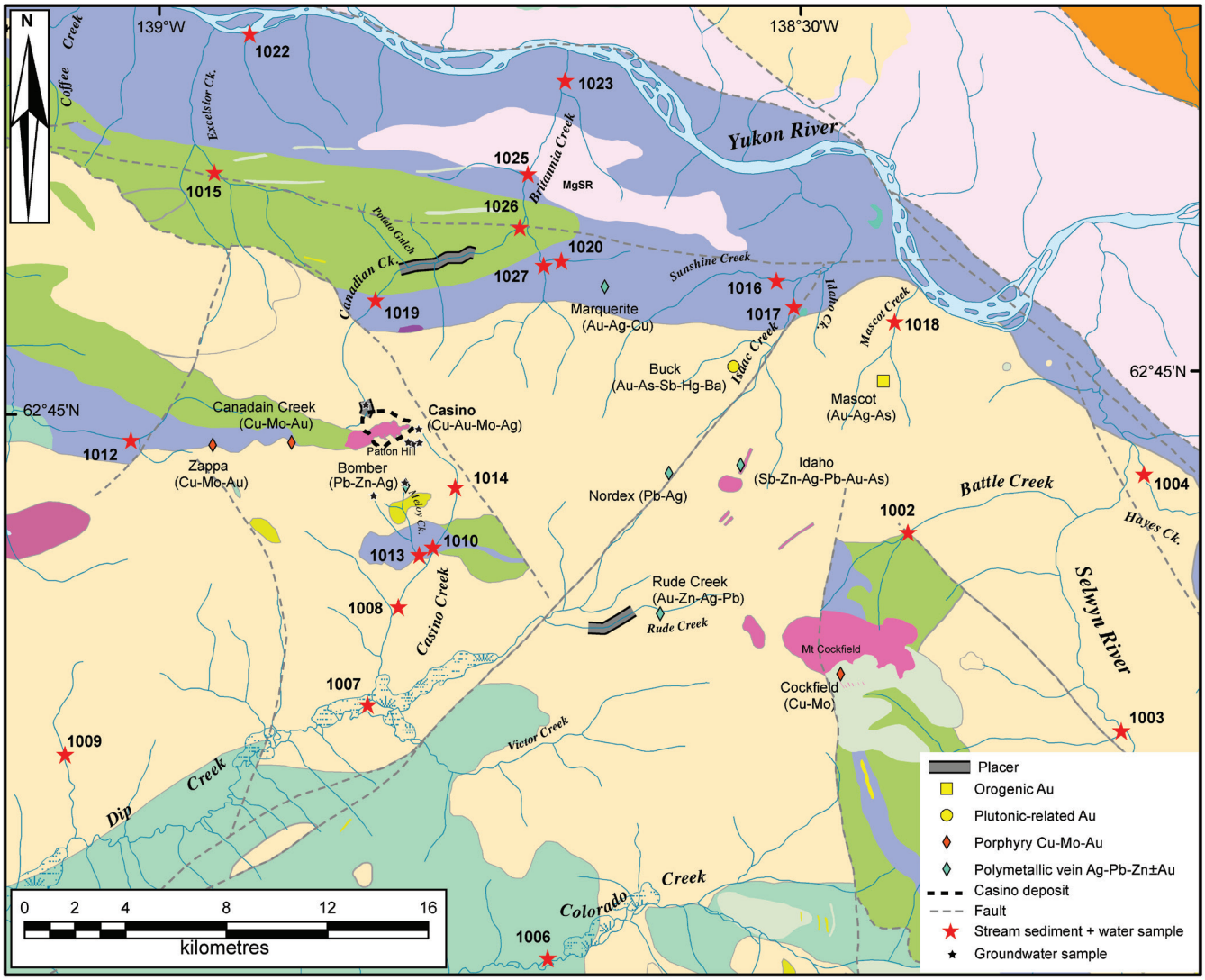

Bedrock Geology

PALEOCENE TO LOWER EOCENE
- RHYOLITE CREEK: rhyolite and dacite
- RHYOLITE CREEK: andesite

LATE CRETACEOUS
- PROSPECTOR MOUNTAIN SUITE: syenite
- CASINO SUITE: quartz-feldspar porphyry

MID-CRETACEOUS
- WHITEHORSE SUITE: granodiorite, diorite
- WHITEHORSE SUITE: quartz monzonite, granite, leucogranite
- MOUNT NANSEN: andesite to dacite flows

UPPER CRETACEOUS
- CARMACKS: augite-olivine basalt and breccia
- CARMACKS: andesite, porphyry
- CARMACKS: sandstone, pebble conglomerate, shale, tuff, coal

LATE TRIASSIC TO EARLY JURASSIC
- MINTO SUITE: granodiorite, gneissic schlieren

LATE TRIASSIC
- STIKINE SUITE: gabbroic Hbl orthogneiss

MIDDLE TO LATE PERMIAN
- SULPHUR CREEK SUITE: granite, metaporphyry
- KLONDIKE SCHIST: qtz-ms-chl schist

MISSISSIPPIAN
- SIMPSON RANGE SUITE: metagranodiorite, metadiorite, metatonalite

DEVONIAN, MISSISSIPPIAN, AND(?) OLDER
- FINLAYSON: intermediate to mafic volcanic and volcaniclastic rocks
- FINLAYSON: carbonaceous metasedimentary rocks, metachert
- FINLAYSON: ultramafic rocks, serpentinite; metagabbro

LATE DEVONIAN TO MISSISSIPPIAN
- MT BAKER SUITE: gneissic granodiorite, diorite, monzogranite, gabbro, minor pyroxenite

ORDOVICIAN TO LOWER DEVONIAN
- SCOTTIE CREEK: quartzite, Qtz-Ms-Bt±Grt schist

NEOPROTEROZOIC AND PALEOZOIC
- SNOWCAP: quartzite, psammite, pelite, marble; minor greenstone and amphibolite
- SNOWCAP: marble

Figure 2. Map of the Casino deposit area showing local bedrock geology (Yukon Geological Survey, 2015b), locations of mineral occurrences (Yukon Geological Survey, 2011a, b, c, 2013a, b, 2015a, 2017, 2018a, b, c, d, e), stream sediment and water sample sites (red stars), and groundwater sample sites (black stars). Sample numbers are listed in black beside each site.

of the Snowcap assemblage of metamorphosed sedimentary and minor volcanic rocks, which is unconformably overlain by the Finlayson, Klinkit, and Klondike assemblages that are predominantly composed of arc metavolcanic rocks and associated metasedimentary rocks (Colpron et al., 2006, 2016; Ryan et al., 2013).

The bedrock geology of the deposit and surrounding area is briefly summarized in this paper based on detailed descriptions by Archer and Main (1971), Godwin (1975, 1976), Bower et al. (1995), Ryan et al. (2013), Casselman and Brown (2017), and Yukon Geological Survey (2015b, 2018c). The Casino deposit is classified as a calc-alkaline porphyry deposit and is centred on the Patton porphyry, a Late Cretaceous (74–72 Ma) stock that intrudes the Mesozoic Dawson Range batholith and Paleozoic Yukon Crystalline Complex schist and gneiss. The intrusion of the small porphyry into these older rocks caused brecciation along its contacts. The porphyry is locally mineralized and is surrounded by a potassic-altered intrusion breccia at its outer contacts. Elsewhere, the porphyry consists of discontinuous dykes (up to tens of metres wide) that cut the porphyry and Dawson Range batholith. The overall composition of the porphyry is rhyodacite, with dacite phenocrysts and a quartz latite matrix.

Primary copper, gold, and molybdenum mineralization was deposited from hydrothermal fluids in the contact breccias and fractured wall rocks and consists of pyrite, chalcopyrite, molybdenite, and minor hübnerite (manganese-tungsten oxide). The primary mineralization is concentrated in the phyllic zone and surrounded by weakly developed argillic and propylitic alteration zones. Grades decrease away from the contact zone toward the centre of the stock and outward into the wall rocks.

Godwin (1975, 1976) suggested that the warm and wet climate of the Paleogene (Zachos et al., 2001; Moran et al., 2006; Vavrek et al., 2012) is the likely timeframe for supergene enrichment of the deposit. The deep weathering profile is largely intact because minimal to no glacial erosion of the region occurred during the last 2 000 000 y (Bond and Lipovsky, 2011, 2012a, b). Thus, the deposit has well-formed zonation consisting of a leached cap, supergene oxide mineralization, supergene sulfide mineralization, and hypogene (primary) mineralization. The leached cap averages 70 m thick, is enriched in gold and depleted in copper, and consists primarily of boxwork textures filled with jarosite, limonite, goethite, and hematite. The deep weathering has obliterated bedrock textures and replaced most minerals with clay. The supergene oxide zone consists of a few isolated lenses within the leached cap and is thought to have formed by more recent fluctuations in the water table. It is rich in copper and contains chalcanthite, malachite, and brocanthite along with minor cuprite, azurite, tenorite, neotocite, and trace molybdenite as coatings on fractures and in vugs. The supergene sulfide zone underlies the leached cap, averages 60 m thick, and outcrops at surface in places. It has Cu grades commonly almost double those in the hypogene zone and contains pyrite, chalcopyrite, bornite, and tetrahedrite that may be altered along grain boundaries to chalcocite, digenite, or covellite, as well as molybdenite that is locally altered to ferrimolybdite. Hypogene mineralization underlies the supergene sulfide zone and consists of pyrite, chalcopyrite, molybdenite, sphalerite, bornite, and tetrahedrite. In the hypogene zone, gold occurs as discrete grains (50–70 µm) in quartz and as inclusions (1–15 µm) in pyrite and chalcopyrite. On the eastern and northern flanks of the deposit, the supergene oxide zone is absent, the other zones are thinner, and the hypogene zone is closest to the surface (<25 m). Potential indicator minerals of the deposit are listed in Table 1.

Mineral occurrences near the Casino deposit are shown in Figure 2. They include porphyry Cu-Mo-Au occurrences 20 km to the southeast on Mount Cockfield (e.g. Cockfield; Yukon Geological Survey, 2018d) and 3 to 6 km west of the Casino deposit (Canadian Creek, Zappa; Yukon Geological Survey, 2018b, e). Additional polymetallic vein occurrences are located 10 km to the northeast (Marquerite; Yukon Geological Survey, 2013b), 10 km to the east (Nordex and Idaho; Yukon Geological Survey, 2011a, b), and 12 km to the southeast (Rude Creek; Yukon Geological Survey, 2011c) of Casino. Two gold occurrences have been reported 13 to 16 km east-northeast of the deposit (Buck and Mascot; Yukon Geological Survey, 2013a, 2015a).

Surficial geology

The surficial geology of the Casino area is summarized below from maps and reports by Duk-Rodkin (2001), Huscroft (2002a, b, c), Duk-Rodkin et al. (2002, 2004), Bond and Sanborn (2006), Jackson et al. (2009), Bond and Lipovsky (2011, 2012a, b), Lipovsky and Bond (2012), and McKillop et al. (2013). The deposit is in the northern Dawson Range, a series of broad ridges and summits that vary in elevation from approximately 1000 to 1800 m a.s.l. and comprise the south part of the Klondike Plateau physiographic region (Bostock, 1970; Mathews, 1986). The highest peaks in the study area are an unnamed peak (1672 m a.s.l.), 3 km to the northwest of Patton Hill (the highest point of the Patton porphyry intrusion, approximately 1432 m a.s.l.), and Mount Cockfield (1856 m a.s.l.), 20 km to the southeast (Fig. 2). The landscape is largely unglaciated. Bedrock outcrop and tors (rocky peaks) are common along the ridges and summits and have disintegrated in situ through mechanical (freeze-and-thaw) and/or chemical weathering. Surficial material in upland areas flanking ridges and summits consists of colluvium and weathered bedrock intermixed with variable amounts of loess. Material moves downslope by gravity-driven processes — creep, solifluction, landslides, and snow avalanches — and eventually into local creeks. Lower lying areas are covered with loess.

Table 1. Potential indicator minerals of the Casino porphyry Cu-Au-Mo deposit, summarized from deposit descriptions by Bostock (1959), Archer and Main (1971), Godwin (1975), Bower et al. (1995), Casselman and Brown (2017), and Huss et al. (2013), and indicator minerals found in stream-sediment samples in this study.

Mineral	Interpretation	Formula	Specific gravity	Hardness	In bedrock HMC in this study	In stream HMC in this study	First reported presence in deposit
Hematite	Potassic alteration	Fe_2O_3	5.3	6.5	No	Yes	Godwin (1975)
Magnetite	Potassic alteration	Fe_3O_4	5.1–5.2	5.5–6	Yes	Yes	Godwin (1975)
Anhydrite	Potassic alteration	$CaSO_4$	2.96–2.98	3.5	No	No	Godwin (1975)
Tourmaline	Potassic alteration	$NaMg_3Al_6(BO_3)_3Si_6O_{18}(OH)_4$	2.98–3.2	7–7.5	Yes	Yes	Godwin (1975)
Ankerite	Potassic alteration	$Ca(Fe,Mg,Mn)(CO_3)_2$	3–3.1	3.5–4	No	No	Godwin (1975)
Pyrite	Potassic alteration	FeS_2	5–5.0	6.5	Yes	Yes	Godwin (1975)
Chalcopyrite	Potassic alteration	$CuFeS_2$	4.1–4.3	3.5	Yes	Yes	Godwin (1975)
Molybdenite	Potassic alteration	MoS_2	5.5	1.0	Yes	Yes	Godwin (1975)
Sphalerite	Potassic alteration	(Zn,Fe)S	3.9–4.2	3.5–4	No	Yes	Godwin (1975)
Bornite	Potassic alteration	Cu_5FeS_4	4.9–5.3	3	No	No	Godwin (1975)
Jarosite	Potassic alteration	$KFe_3(SO_4)_2(OH)_6$	2.9–3.3	2.5–3.5	No	Yes	Godwin (1975)
Tourmaline	Phyllic alteration	$NaMg_3Al_6(BO_3)_3Si_6O_{18}(OH)_4$	2.98–3.2	7–7.5	Yes	Yes	Archer and Main (1971)
Titanite	Phyllic alteration	$CaTiSiO_5$	3.4–3.56	5–5.5	No	Yes	Huss et al. (2013)
Pyrite	Phyllic alteration	FeS_2	5–5.0	6.5	Yes	Yes	Archer and Main (1971)
Chalcopyrite	Phyllic alteration	$CuFeS_2$	4.1–4.3	3.5	Yes	Yes	Archer and Main (1971)
Molybdenite	Phyllic alteration	MoS_2	5.5	1.0	Yes	Yes	Archer and Main (1971)
Hematite	Phyllic alteration	Fe_2O_3	5.3	6.5	No	Yes	Archer and Main (1971)
Magnetite	Phyllic alteration	Fe_3O_4	5.1–5.2	5.5–6	Yes	Yes	Godwin (1975)
Jarosite	Phyllic alteration	$KFe_3(SO_4)_2(OH)_6$	2.9–3.3	2.5–3.5	No	Yes	Archer and Main (1971)
Epidote	Propylitic alteration	$Ca_2(FeAl)_3(SiO_4)_3(OH)$	3.3–3.6	7	Yes	Yes	Godwin (1975)
Pyrite	Propylitic alteration	FeS_2	5–5.0	6.5	Yes	Yes	Godwin (1975)
Limonite	Leached cap	$FeO(OH)•nH_2O$	2.7–4.3	4–5.5	No	No	Archer and Main (1971)
Jarosite	Leached cap	$KFe_3(SO_4)_2(OH)_6$	2.9–3.3	2.5–3.5	No	Yes	Archer and Main (1971)
Plumbojarosite	Leached cap	$PbFe_6(SO_4)_4(OH)_{12}$	3.6–3.67	1.5–2	No	Yes	Huss et al. (2013)
Beudantite	Leached cap	$PbFe_3(AsO_4)(SO_4)(OH)_6$	4.1–4.3	4	No	Yes	Huss et al. (2013)
Pyrolusite	Leached cap	MnO_2	4.4–5.06	6–6.5	No	Yes	Huss et al. (2013)
Goethite	Leached cap	FeO(OH)	3.3–4.3	5–5.5	Yes	Yes	Godwin (1975)
Hematite	Leached cap	Fe_2O_3	5.3	6.5	No	Yes	Archer and Main (1971)

Table 1 (cont.). Potential indicator minerals of the Casino porphyry Cu-Au-Mo deposit, summarized from deposit descriptions by Bostock (1959), Godwin (1975), Bower et al. (1995), Casselman and Brown (2017), and Huss et al. (2013), and indicator minerals found in stream-sediment samples in this study.

Mineral	Interpretation	Formula	Specific gravity	Hardness	In bedrock HMC in this study	In stream HMC in this study	First reported presence in deposit
Ferrimolybdite	Leached cap	$Fe_2(MoO_4)_3•8(H_2O)$	4–4.5	2.5–3	No	No	Godwin (1975)
Chalcanthite	Supergene oxide	$Cu(SO_4)•5(H_2O)$	2.12–2.3	2.5	No	No	Godwin (1975)
Brochantite	Supergene oxide	$Cu_4(SO_4)(OH)_6$	3.97	3.5–4	No	No	Godwin (1975)
Malachite	Supergene oxide	$Cu_2(CO_3)(OH)_2$	3.6–4	3.5–4	No	No	Godwin (1975)
Azurite	Supergene oxide	$Cu_3(CO_3)_2(OH)_2$	3.77–3.89	3.5–4	No	No	Godwin (1975)
Tenorite	Supergene oxide	CuO	6.5	3.5–4	No	No	Godwin (1975)
Cuprite	Supergene oxide	Cu_2O	6.1	3.5–4	No	No	Bower et al. (1995)
Neotocite	Supergene oxide	$(MnFe)SiO_3•(H_2O)$	2.8	3–4	No	No	Godwin (1975)
Native copper	Supergene oxide	Cu	8.94–8.95	2.5–3	No	No	Godwin (1975)
Digenite	Supergene sulfide	Cu_9S_5	5.6	2.5–3	No	No	Archer and Main (1971)
Chalcocite	Supergene sulfide	Cu_2S	5.5–5.8	2.5–3	No	No	Archer and Main (1971)
Covellite	Supergene sulfide	CuS	4.6–4.76	1.5–2	No	No	Archer and Main (1971)
Enargite	Supergene sulfide	Cu_3AsS_4	4.4–4.5	3	No	No	Casselman and Brown (2017)
Bornite	Supergene sulfide	Cu_5FeS_4	4.9–5.3	3	No	No	Huss et al. (2013)
Pyrite	Hypogene mineralization	FeS_2	5–5.0	6.5	Yes	Yes	Archer and Main (1971)
Chalcopyrite	Hypogene mineralization	$CuFeS_2$	4.1–4.3	3.5	Yes	Yes	Archer and Main (1971)
Molybdenite	Hypogene mineralization	MoS_2	5.5	1.0	Yes	Yes	Archer and Main (1971)
Sphalerite	Hypogene mineralization	(Zn,Fe)S	3.9–4.2	3.5–4	No	Yes	Godwin (1975)
Bornite	Hypogene mineralization	Cu_5FeS_4	4.9–5.3	3	No	No	Godwin (1975)
Gold	Hypogene mineralization	Au	16–19.3	2.5–3	Yes	Yes	Archer and Main (1971)
Galena	Hypogene mineralization	PbS	7.2–7.6	2.5	No	No	Archer and Main (1971)
Tetrahedrite	Hypogene mineralization	$Cu_9Fe_3Sb_4S_{13}$	4.6–5.2	3.5–4	No	No	Bower et al. (1995)
Bismuthinite	Hypogene mineralization	Bi_2S_3	6.8–7.2	2.0	No	Yes	Huss et al. (2013)
Ankerite	Hypogene mineralization	$Ca(Fe,Mg,Mn)(CO_3)_2$	3–3.1	3.5–4	No	No	Bower et al. (1995)
Barite	Polymetallic veins	$BaSO_4$	4.5	3–3.5	Yes	Yes	Archer and Main (1971)
Sphalerite	Polymetallic veins	(Zn,Fe)S	3.9–4.2	3.5–4	No	Yes	Archer and Main (1971)
Ag-rich galena	Polymetallic veins	PbS	7.2–7.6	2.5	No	No	Archer and Main (1971)
Scheelite	Polymetallic veins	$CaWO_4$	5.9–6.1	4–5	No	Yes	Archer and Main (1971)

Table 1 (cont.). Potential indicator minerals of the Casino porphyry Cu-Au-Mo deposit, summarized from deposit descriptions by Bostock (1959), Godwin (1975), Bower et al. (1995), Casselman and Brown (2017), and Huss et al. (2013), and indicator minerals found in stream-sediment samples in this study.

Mineral	Interpretation	Formula	Specific gravity	Hardness	In bedrock HMC in this study	In stream HMC in this study	First reported presence in deposit
Chalcopyrite	Polymetallic veins	$CuFeS_2$	4.1–4.3	3.5	Yes	Yes	Archer and Main (1971)
Pyrite	Polymetallic veins	FeS_2	5–5.0	6.5	Yes	Yes	Archer and Main (1971)
Gold	Placer: upper Canadian Creek	Au	16–19.3	2.5–3	Yes	Yes	Bostock (1959)
Ferberite	Placer: upper Canadian Creek	$Fe(WO_4)$	7.5	4.5	No	No	Bostock (1959)
Scheelite	Placer: upper Canadian Creek	$CaWO_4$	5.9–6.1	4–5	No	Yes	Bostock (1959)
Molybdenite	Placer: upper Canadian Creek	MoS_2	5.5	1.0	Yes	Yes	Bostock (1959)
Cassiterite	Placer: upper Canadian Creek	SnO_2	6.8–7	6–7	No	No	Bostock (1959)
Tourmaline	Placer: upper Canadian Creek	$NaMg_3Al_6(BO_3)_3Si_6O_{18}(OH)_4$	2.98–3.2	7–7.5	Yes	Yes	Bostock (1959)
Titanite	Placer: upper Canadian Creek	$CaTiSiO_5$	3.4–3.56	5–5.5	No	Yes	Bostock (1959)
Hematite	Placer: upper Canadian Creek	Fe_2O_3	5.3	6.5	No	Yes	Bostock (1959)
Magnetite	Placer: upper Canadian Creek	Fe_3O_4	5.1–5.2	5.5–6	Yes	Yes	Bostock (1959)

HMC: heavy mineral concentrate

Isolated alpine glaciers existed on Mount Cockfield during the middle Pleistocene Reid glaciation, extending west into the headwaters and a tributary valley of Victor and Colorado creeks and east into an unnamed tributary that drains into the Selwyn River (Bond and Lipovsky, 2012a). Glacial sediments (end moraines) and cirques are present on the east flank of Mount Cockfield; stream sediments in the creeks draining this east flank will be derived, in part, from the glacial sediments. Evidence of past glaciation also exists in the headwaters of Canadian Creek, immediately northwest of Patton Hill, where cirques formed during early Pleistocene (pre-Reid) glaciation (Duk-Rodkin et al., 2002; Bond and Lipovsky, 2012a).

Permafrost is discontinuous and is most common on north-facing slopes and valley bottoms that are covered by thick, fine-grained colluvium and organic veneers (Smith et al., 2009; Bond and Lipovsky, 2011). The presence of permafrost is indicated by features such as solifluction lobes, pingos, and thermokarst features.

First- and second-order streams (e.g. Casino Creek) occur in narrow V-shaped valleys and contain subangular to subrounded gravel to boulders composed of locally derived bedrock. Higher order streams occur in broader valleys and are filled with more distally derived colluvium, loess, and rounded gravel (e.g. Dip Creek, Colorado Creek). Bond and Lipovsky (2012a) reported that understanding the relationship between valley morphology and the variable texture and sources of fluvial sediments is important when sampling for and interpreting stream silt geochemical surveys. Because loess content in fluvial sediments is variable, Bond and Lipovsky (2012a) recommended that stream samples ideally be collected from high-energy streams in narrow valleys where the loess content is lowest.

Previous stream-sediment geochemical surveys

Archer and Main (1971) reported that, at the time of discovery, the Casino deposit had an obvious geochemical signature in stream silts (Cu, Mo, Au, and Ag) and waters (Cu) overlying the deposit. Subsequent reconnaissance-scale stream silt and water sampling in Yukon by the GSC (Geological Survey of Canada, 1987; 19 elements in <0.177 mm silt using 3:1 HNO_3:HCl, pH, 2 elements in water) and subsequent reanalysis of these GSC stream-sediment samples (53 elements in <0.177 mm silt using 1:3 HNO_3:HCl; Jackaman, 2011; Yukon Geological Survey, 2016; Mackie et al., 2017; Arne et al., 2018) show an obvious multi-element geochemical anomaly (Ag, Cu, Mo, Pb, Sb, W) in the local creeks draining the Casino deposit.

The Yukon Geological Survey collected a few isolated heavy mineral samples from local creeks while mapping the surficial geology of the Casino area. They reported the presence of gold grains in two of their nine samples: one sample from upper Casino Creek and one sample from Rude Creek (Bond and Lipovsky, 2012a, b; Lipovsky and Bond, 2012).

Chapman et al. (2014, 2018) compared lode gold signatures in the Casino deposit and large (100 kg) bulk gravel samples from known placer occurrences along Casino, Canadian, and Rude creeks (Fig. 2). They reported that gold grains in the Casino deposit bedrock samples were between 50 to 1000 µm (long axis of grains) and in gravel samples between 500 to 2000 µm. Using gold grain trace-element chemistry and inclusion compositions, they concluded that the large gold placer occurrence in the middle reaches of Canadian Creek contained a mixture of gold derived from two sources: the Casino porphyry deposit and unknown epithermal mineralization. Barkov et al. (2008) reported the presence of several indicator minerals in a heavy mineral concentrate (HMC) sample from the same large placer occurrence on Canadian Creek, below the confluence with Potato Gulch (Fig. 2). In addition to tin-rich hematite, they recovered ferberite, hübnerite, bismuthinite, daubréeite, tetradymite, and goethite in the sample. In the same placer sample, Fedortchouk and LeBarge (2008) reported the presence of one grain of platinum-iron alloy.

METHODS

Sample collection

A total of 24 stream-silt and water samples and 22 heavy mineral samples were collected at 22 sites (Fig. 2) around the Casino deposit in September 2017 using GSC protocols established by Friske and Hornbrook (1991) and described in detail by Day et al. (2013) and Plouffe et al. (2013). Field observations were digitally recorded on a tablet using a standard form developed jointly by the GSC and the Northwest Territories Geological Survey. Field data and photographs of all stream-sediment sample sites are included in McCurdy et al. (2019).

At each site, two 60 mL water samples were collected in the mid-channel of local creeks: i) a filtered, acidified sample ('FA') and ii) a filtered, unacidified sample ('FU'). On site, each 60 mL water sample was filtered through a 0.45 µm disposable filter into a triple-rinsed 60 mL Nalgene® bottle. In situ stream water measurements included temperature, pH, conductivity, dissolved oxygen (DO), and oxidation-reduction potential (ORP) with automatic temperature compensation for pH and DO. After the water samples were collected, approximately 1 to 2 kg of silt and fine sand was collected by hand from various points in the active channel while moving upstream, over a distance of 5 to 15 m. A third bulk heavy mineral stream-sediment sample of between 8 and 16 kg was collected from large gravel bars, boulder traps, or tiny pools of sediment in rocky narrow streams. Samples were wet sieved onsite to remove the fragments greater than 2 mm.

Nine groundwater samples were collected by Western Copper and Gold Corporation during the same time period from monitoring wells in eight locations (Fig. 2). Samples for total metals analyses were collected in 120 mL acid-washed plastic bottles and preserved in the field with laboratory-supplied, ultrapure HNO_3. Samples for dissolved metal analyses were filtered through a 0.45 µm disposable filter in the field and preserved with ultrapure HNO_3 immediately after filtration. Western Copper and Gold Corporation shared these water samples with the GSC after splits were analyzed at a commercial laboratory.

Heavy mineral sample processing

The stream-sediment heavy mineral samples were weighed and processed at Overburden Drilling Management Ltd. (ODM), Ottawa, Ontario, for recovery of HMCs using methods outlined by Plouffe et al. (2013). There were 22 stream-sediment samples plus 3 blank quality control (QC) samples (for a total of 25 samples) processed. Samples were first passed across a shaking table to prepare a less than 2.0 mm preconcentrate. The preconcentrate was micropanned to recover and count fine-grained gold, sulfide minerals, and other indicator minerals. Gold grain size and shape characteristics were classified using DiLabio's (1990) scheme (pristine-modified-reshaped) adapted for fluvial transport distance (Averill, pers. comm., 2020) and then all panned grains were returned to the concentrate. Gold grain counts reported in this paper reflect this stage of the sample processing procedure. The preconcentrate was then subjected to two heavy-liquid separations to produce 2.8 to 3.2 specific gravity (SG) and greater than 3.2 SG non-ferromagnetic HMCs for visual identification of indicator minerals. Before examination, the grains were subjected to an oxalic acid wash to facilitate mineral identification. The 0.25 to 0.5, 0.5 to 1.0, and 1.0 to 2.0 mm non-ferromagnetic greater than 3.2 SG fractions and the 0.25 to 0.5 mm non-ferromagnetic 2.8 to 3.2 SG fraction of bedrock and stream-sediment samples were examined by ODM, potential indicator minerals were counted, and selected grains were removed for chemical analysis. The mass of all fractions produced and abundance of indicator minerals in the 22 stream-sediment and 3 QC samples, along with sample processing flow charts, are reported by McClenaghan et al. (2020).

Geochemical analysis

Stream-silt samples were air dried at less than 40°C, disaggregated, and sieved to recover the less than 0.177 mm fraction for geochemical analysis. Geochemical analytical data quality was monitored by inserting CANMET Certified Reference Material (CRM) Stream Sediment-1

(STSD-1) and Stream Sediment-4 (STSD-4; Lynch, 1990, 1999; CANMET, 2020) and analytical duplicate samples into each block of 20 samples. A 30 g aliquot of each sample was tested for 35 elements by instrumental neutron activation analysis (INAA) at Maxxam Analytics (formerly Becquerel Labs), Mississauga, Ontario. A separate 0.5 g aliquot was analyzed for 65 elements at Bureau Veritas Commodities Canada (BVCC), Vancouver, British Columbia, using a modified aqua regia solution (1:1 HCl:HNO_3) and detection by inductively coupled plasma mass spectrometry (ICP-MS). Lead collection fire assay was used to concentrate Au, Pt, and Pd from a separate 30 g aliquot into a silver doré bead that was then digested in HNO_3, and the solution was analyzed by ICP-MS. Stream silt geochemical data for all methods and the evaluation of quality-control data were reported by McCurdy et al. (2019). A separate split of dried, unsieved stream silt was analyzed in a 4 dram (approximately 15 mL) plastic vial covered with 4 µm Prolene® film using a hand-held portable X-ray fluorescence (pXRF) unit at the GSC's Inorganic Geochemistry Research Laboratory (IGRL), Ottawa, Ontario. Samples were analyzed twice and the mean values for each sample were used for data interpretations (McCurdy et al., 2019).

Streamwater samples collected by the GSC were kept cool and in the dark until shipment to the IGRL, where they were acidified within 48 h of arrival with 0.5 mL 8M ultrapure HNO_3. Anion analysis (FU series) was completed using a Dionex™ ICS 2100 ion chromatograph fitted with an AS-AP autosampler. Acidified and filtered (FA series) streamwater samples were analyzed for trace metals and major elements using a quadrupole inductively coupled plasma–mass spectrometer (ICP-MS). Major element analysis was performed using an inductively coupled plasma–optical emission spectrometer (ICP-OES). The groundwater samples from Western Copper and Gold were also analyzed at the IGRL using the same methods. In addition to analyses performed at the GSC, water samples were subsequently analyzed for $\delta^{18}O$, $\delta^{2}H$, $\delta^{34}S_{SO_4}$, and $\delta^{18}O_{SO_4}$ (for samples with sufficient SO_4), $\delta^{65}Cu$, and $^{87}Sr/^{86}Sr$ at the Queen's University Facility for Isotope Research (QFIR).

RESULTS

Stream sediment mineralogy

Grain counts for selected indicator minerals are reported in Table 2 and described below as values normalized to 10 kg of material of less than 2 mm to allow comparison between samples of different mass. Individual mineral distribution maps are included in McClenaghan et al. (2020) and are summarized below. Unless otherwise stated, the results are for the 0.25 to 0.5 mm size HMC fraction.

Stream sediments contain between 0 and 44 gold grains (Fig. 3a) in the pan concentrate fraction. Abundances are highest in samples from Casino Creek on the south side of the deposit and Canadian and Britannia creeks draining the north side of the deposit (Fig. 4). Gold grains in these three creeks range in size from 25 to 1500 µm, with most grains being between 25 and 200 µm in size and modified to reshaped in appearance (Table 3).

Chalcopyrite (Fig. 3b) was recovered from most stream-sediment samples, with the largest number of grains being recovered from sample 1003 (26 grains), downstream of the Cockfield occurrence; sample 1012 (13 grains), downstream of the Zappa occurrence; and sample 1019 (7 grains), downstream of the Casino deposit. Most other stream-sediment samples contained between 0 and 4 grains (Fig. 5). The presence of chalcopyrite is somewhat unexpected because the terrain, except for east of Mount Cockfield, is unglaciated and the deep weathering of bedrock was expected to have destroyed chalcopyrite in rocks exposed at surface.

Pyrite (Fig. 3c) was recovered from all but two stream-sediment samples. It is most abundant in sample 1012 (2113 grains) from the creek draining the Zappa occurrence; sample 1003 (397 grains), downstream of the Cockfield occurrence, sample 1004 (194 grains) on Hayes Creek, and sample 1015 (168 grains) on Excelsior Creek, 12 km northwest of the Casino deposit. The highest count in Casino Creek samples is 79 grains (sample 1015).

Molybdenite (Fig. 3d) was recovered from four stream-sediment samples (Table 2): sample 1014 from Casino Creek; sample 1003, downstream of the Cockfield occurrence; sample 1013, approximately 20 km downstream of the deposit in Britannia Creek; and sample 1012, downstream of the Zappa occurrence (Fig. 6).

Low-Fe sphalerite grains were identified in three stream-sediment samples by their honey brown colour (Fig. 3e). Some of the grains appear to be corroded, indicating that they underwent chemical weathering. The grains were recovered from sample 1013 from Meloy Creek, sample 1014 from Casino Creek, and sample 1019 from Canadian Creek (Table 2). In addition to chalcopyrite, pyrite, and sphalerite, a few grains of bismuthinite (Fig. 3f) and arsenopyrite (Fig. 3g) were recovered from samples collected downstream of the Cockfield occurrence.

A few tourmaline grains (Fig. 3h) were recovered from the 2.8 to 3.2 SG fraction of samples from Casino Creek, but the greatest number of grains were recovered farther downstream in Canadian (sample 1026) and Britannia creeks (sample 1025), in creeks downstream of the Cockfield occurrence (samples 1002, 1003), and in Sunshine Creek (sample 1016; *see* Fig. 1 in Beckett-Brown et al., this volume). The presence of tourmaline is obvious throughout the Casino deposit as disseminations, in veins, and in breccias (Beckett-Brown et al., 2019, this volume), thus the recovery of tourmaline from local stream sediments is not surprising.

Scheelite (Fig. 7a, b) is most abundant in stream sediments from Casino and Canadian creeks, downstream of the Cockfield and Zappa occurrences, and on Sunshine Creek.

Table 2. Abundance (grain count) of select indicator minerals in the >3.2 specific gravity (SG) and 2.8 to 3.2 SG 0.25 to 0.5 mm non-ferromagnetic fractions and pan concentrate gold fraction of stream-sediment samples. Counts have been normalized to 10 kg of less than 2 mm (table feed) material.

Sample number	Creek	Gold (pan conc.)	Pyrite	Chalco	Moly	Sphal	Plumb	Beaudan	Pyro	Goethite	Barite	Green epidote	Tur	Scheel	Fluorite	Jarosite SG 2.8–3.2	Tur SG 2.8–3.2
1002	Battle Creek	1	1	2	0	0	1	0	0	407	41	472	0	11	0	163	24
1003	Unnamed creek near Cockfield occurrence	1	397	26	3	0	0	0	0	3311	993	4967	0	26	0	331	26
1004	Hayes Creek	5	194	1	0	0	0	0	0	4651	9302	0	0	2	0	78	0
1006	Colorado Creek	2	0	0	0	0	0	0	0	379	1	0	0	1	0	45	30
1007	Casino Creek	44	13	0	0	0	0	0	0	1007	805	16 308	0	40	0	0	0
1008	Casino Creek	21	4	2	0	0	0	0	0	5825	777	3223	0	4	0	291	4
1009	Unnamed tributary of Dip Creek	1	0	0	0	0	0	0	0	28	0	0	0	0	0	0	0
1010	Casino Creek	8	0	0	0	0	0	1	0	18 349	459	5725	0	37	0	183	11
1012	Unnamed creek near Zappa occurrence	1	2113	13	3	0	0	0	0	141	423	14 085	0	35	0	423	0
1013	Meloy Creek	0	11	4	0	11	86	0	2518	17 986	719	1324	0	2	0	36	0
1014	Casino Creek	1	79	0	1	9	0	0	0	9868	526	3816	0	0	0	132	0
1015	Excelsior Creek	0	168	3	0	0	0	0	0	168	25	65 546	0	1	0	50	2
1016	Sunshine Creek	0	22	1	0	0	0	0	0	1079	7194	45 324	6	36	0	144	360
1017	Isaac Creek	6	3	0	0	0	0	0	0	840	126	7143	0	8	0	0	0
1018	Mascot Creek	3	28	1	0	0	0	0	0	1724	103	4828	0	4	0	0	0
1019	Upper Canadian Creek	28	115	7	0	1	0	0	0	4615	115	19 615	0	23	0	31	0
1020	Unnamed creek near Marquerite occurrence	14	26	0	0	0	0	0	0	34 783	1043	126 086	0	11	0	0	0
1022	Unnamed creek draining into Yukon River	0	63	3	0	0	0	0	0	794	31746	126 984	24	10	2	40	317
1023	Britannia Creek	2	122	1	1	0	0	0	0	3659	366	207 317	0	0	1	183	0
1025	Britannia Creek	19	35	0	0	0	0	0	0	13 274	44	145 133	2	2	0	1327	88
1026	Lower Canadian Creek	6	15	2	0	0	0	0	0	7692	0	153 846	7	2	0	1231	62
1027	Unnamed creek near Marquerite occurrence	0	2	0	0	0	0	0	0	4110	1712	22 603	0	3	0	27	0

Abbreviations: Chalco: chalcopyrite; Moly: molybdenite; Sphal: sphalerite; Plumb: plumbojarosite; Beudan: beaudantite; Pyro: pyrolusite; Scheel: scheelite; Tur: tourmaline
SG: specific gravity; HMC: heavy mineral concentrate

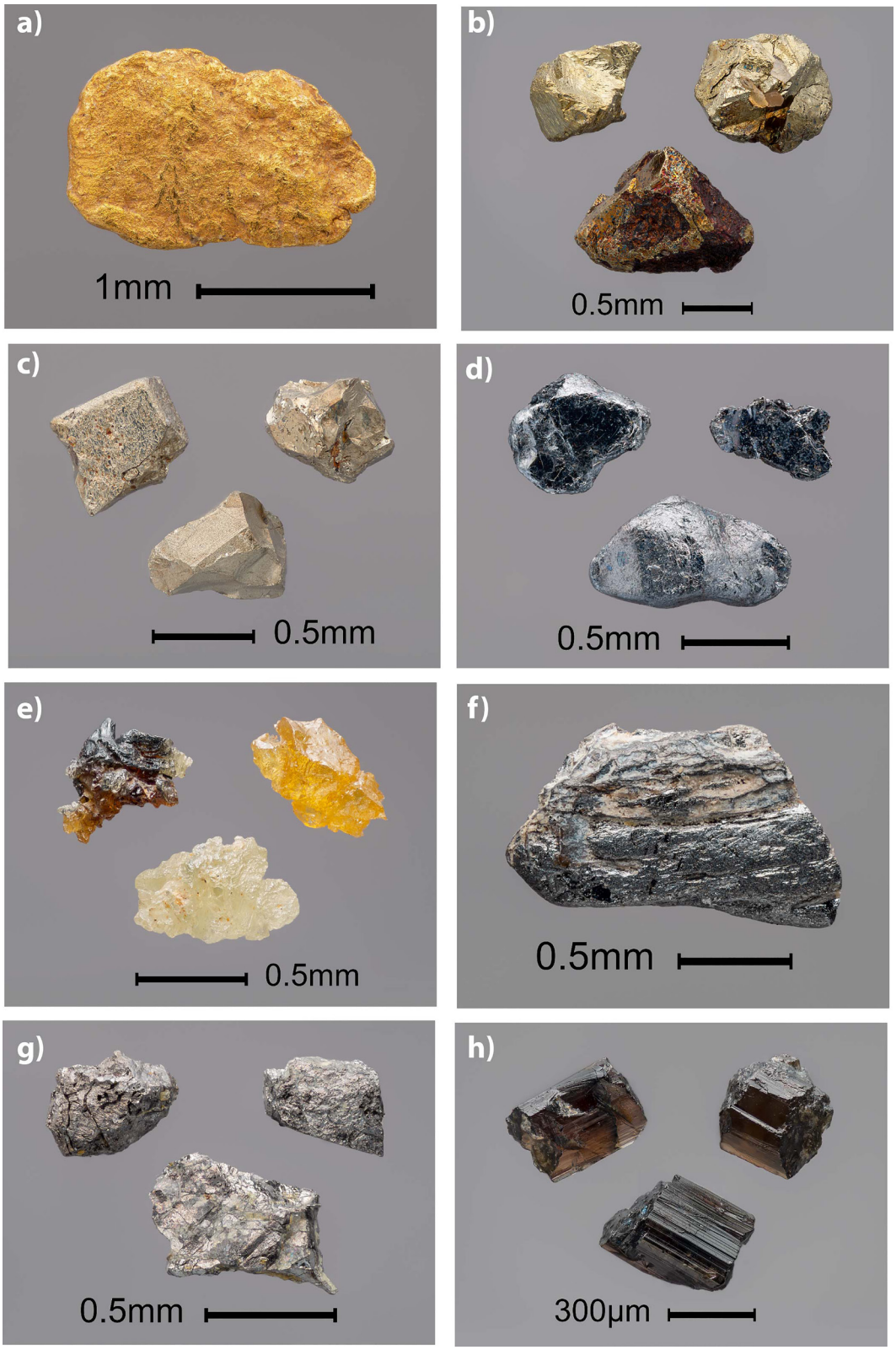

Figure 3. Colour photographs of indicator minerals recovered from the heavy mineral fraction of stream sediments collected around the Casino deposit: **a)** gold; **b)** chalcopyrite; **c)** pyrite; **d)** molybdenite; **e)** sphalerite; **f)** bismuthinite; **g)** arsenopyrite; and **h**) tourmaline (mid-density fraction). Photographs courtesy of Michael J. Bainbridge Photography.

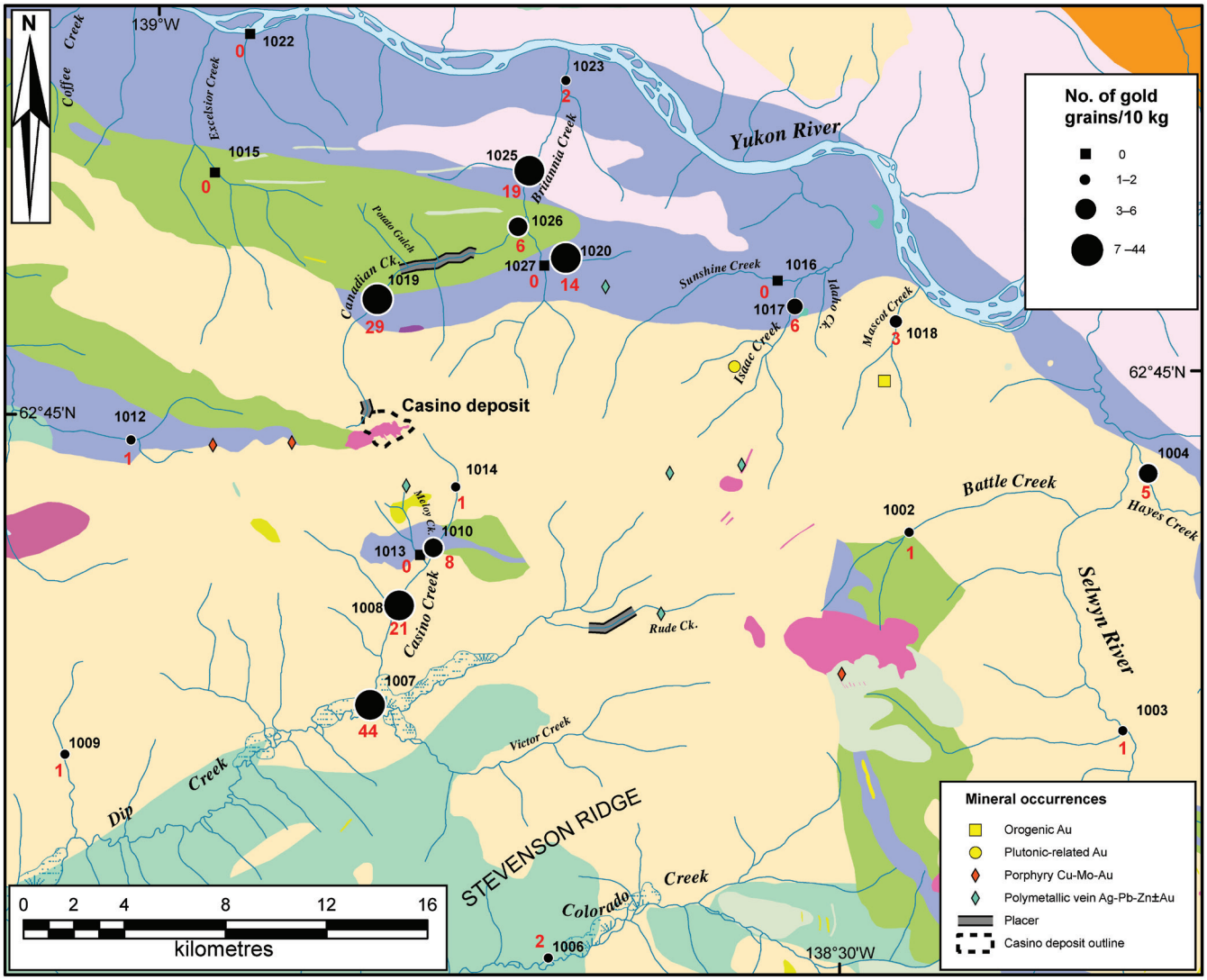

Figure 4. Gold grain abundance in the pan concentrate fraction of heavy mineral stream-sediment samples collected in 2017 (n = 22) in the Casino deposit area. Samples numbers are labeled in black and abundance values are in red. *See* Figure 2 for bedrock geology legend.

Table 3. Abundance (count), size, and shape of gold grains in stream-sediment samples collected from creeks draining the Casino deposit.

Sample	Creek	Mass of <2 mm fraction (kg)	Grain dimensions		Grain shape			Total no. of grains
			Width (µm)	Length (µm)	Reshaped	Modified	Pristine	
1007	Casino	14.9	25	25		1		65
			25	50	1	1	1	
			25	75	1	1		
			50	50	3	1		
			50	75			1	
			50	100	2	1		
			50	150	2			
			75	75	1	2		
			75	100	4	1		
			75	125	3	2		
			75	150	2	2		
			100	100	4			
			100	125	2			
			100	150	3	1		
			100	200	2	1		
			125	125	2	1		
			125	175	3	2		
			150	150	1	1		
			150	200	2			
			150	300	2			
			150	400	3			
			200	200	1			
			250	250	1			
1008	Casino	10.3	25	25	1	2		22
			25	50		1	1	
			50	50		1		
			50	75	1	1		
			50	100		1		
			75	75	1	2		
			75	100	1	1		
			75	125	1			
			100	150		1		
			100	200	2			

Table 3 (cont.). Abundance (count), size, and shape of gold grains in stream-sediment samples collected from creeks draining the Casino deposit.

Sample	Creek	Mass of <2 mm fraction (kg)	Grain dimensions		Grain shape			Total no. of grains
			Width (µm)	Length (µm)	Reshaped	Modified	Pristine	
			100	150	1			
			125	175	1			
			150	250	1			
			150	300	1			
1010	Casino	10.9	75	100	1			9
			75	200		1		
			100	125	1			
			100	150	1			
			200	300	1			
			200	350	1			
			250	250	1			
			250	750	1			
			300	900	1			
1013	Meloy	13.9			0			0
1014	Casino	15.2	200	300	1			2
			250	400	1			
1023	Britannia	16.4	75	125		1		3
			75	150		1		
			125	125	1			
1025	Britannia	11.3	25	50		1		21
			50	75	1			
			50	100	1			
			75	125	1			
			100	125	2			
			100	250	1			
			125	125	1			
			125	175	1			
			125	250	1			
			150	175	1			
			175	200	1			
			200	350	1			
			250	250	3			

Table 3 (cont.). Abundance (count), size, and shape of gold grains in stream-sediment samples collected from creeks draining the Casino deposit.

Sample	Creek	Mass of <2 mm fraction (kg)	Grain dimensions		Grain shape			Total no. of grains
			Width (µm)	Length (µm)	Reshaped	Modified	Pristine	
			250	300	1			
			250	350	1			
			250	500	1			
			300	350	1			
			1000	1500	1			
1026	Canadian	13.0	50	100			1	8
			75	125	2	1		
			100	175		1		
			125	125	1			
			125	150	1			
			250	650	1			
1019	Canadian	13.0	25	50		2	2	37
			25	75			1	
			50	50	1	1	1	
			50	75		2		
			50	125		1		
			75	75	1	1		
			75	100	2			
			75	125	4	1		
			75	150		2		
			75	200		1		
			100	100	1			
			100	150	1	1		
			100	200		1		
			125	150	1			
			125	200	1			
			150	300	1			
			150	350	1			
			175	350	1			
			175	400	1			
			200	300	1			
			300	400	1			
			300	500	1			
			500	750	1			

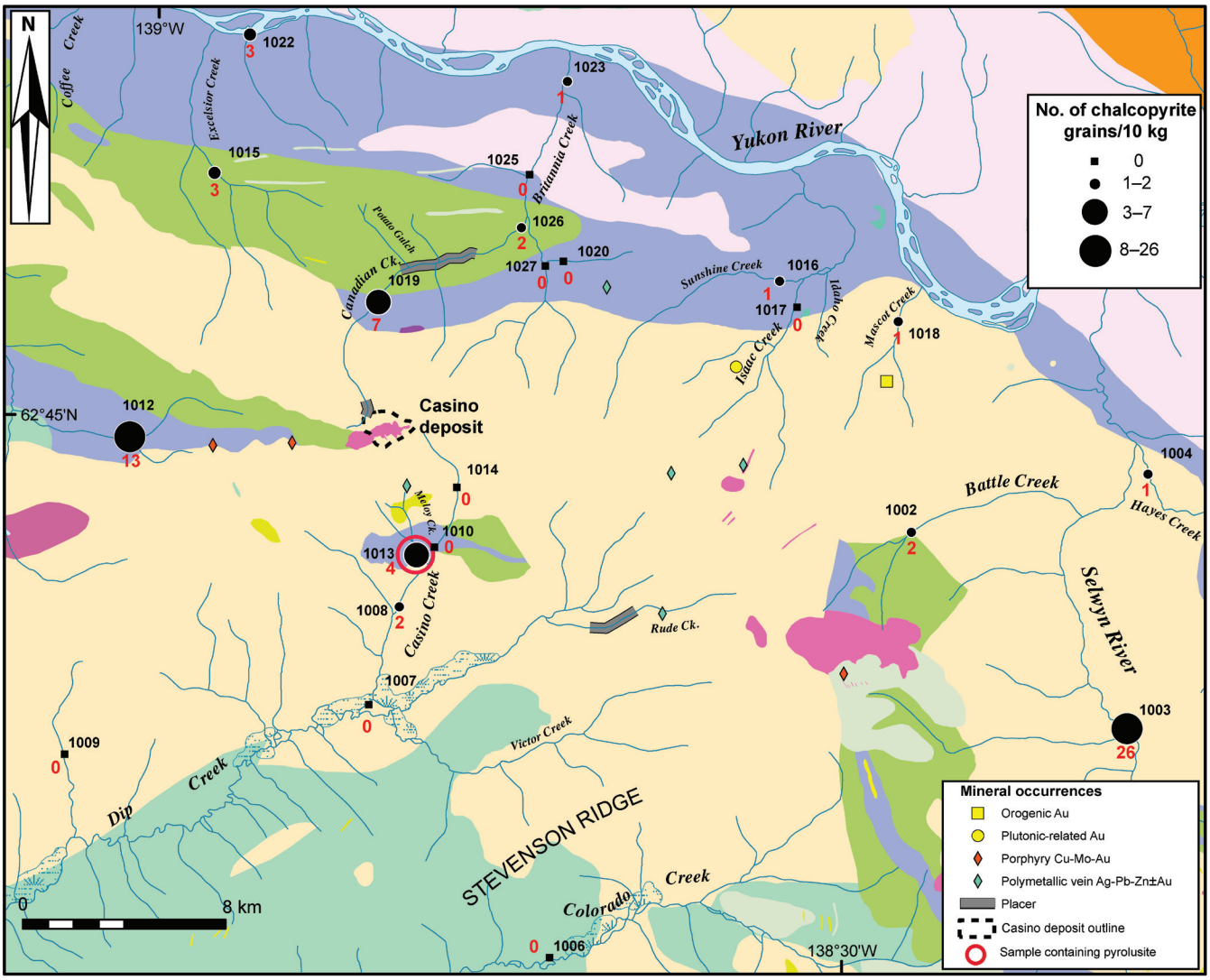

Figure 5. Chalcopyrite abundance in the 0.25 to 0.5 mm heavy mineral fraction of stream-sediment samples collected in 2017 (n = 22) in the Casino deposit area. Location of the sample containing pyrolusite and plumbojarosite grains is indicated by the red circle. Samples numbers are labelled in black and abundance values in red. *See* Figure 2 for bedrock geology legend.

The presence of scheelite was noted in the upper Canadian Creek placer occurrence by Bostock (1959), thus its presence was not unexpected in local stream-sediment samples.

Jarosite was visually identified in the 2.8 to 3.2 SG fraction of stream sediments and is yellowish to light brown (Fig. 7c). Stream-sediment samples 1025 and 1026 from Britannia Creek and lower Canadian Creek contained the most jarosite (1200–1300 grains; Table 2). Samples that contained hundreds of jarosite grains include those from Casino Creek and samples downstream of the Cockfield and Zappa occurrences.

Pyrolusite was visually identified in stream-sediment HMC by its dull, black, amorphous appearance (Fig. 7d) and was confirmed by scanning electron microscopy (SEM). Approximately 2500 grains were recovered from Meloy Creek (sample 1013; Fig. 5). In addition to pyrolusite, approximately 86 grains of plumbojarosite (Fig. 7e) were recovered from the same sample. One plumbojarosite grain was also recovered from sample 1002, downstream of the Cockfield occurrence. Beudantite, a secondary Pb-As sulfate mineral, was identified in sample 1010 from Casino Creek (Table 2). Goethite (Fig. 7f) and hematite were recovered from all but two stream-sediment samples (Table 2). Potential porphyry indicator minerals green epidote (Fig. 7g), barite,

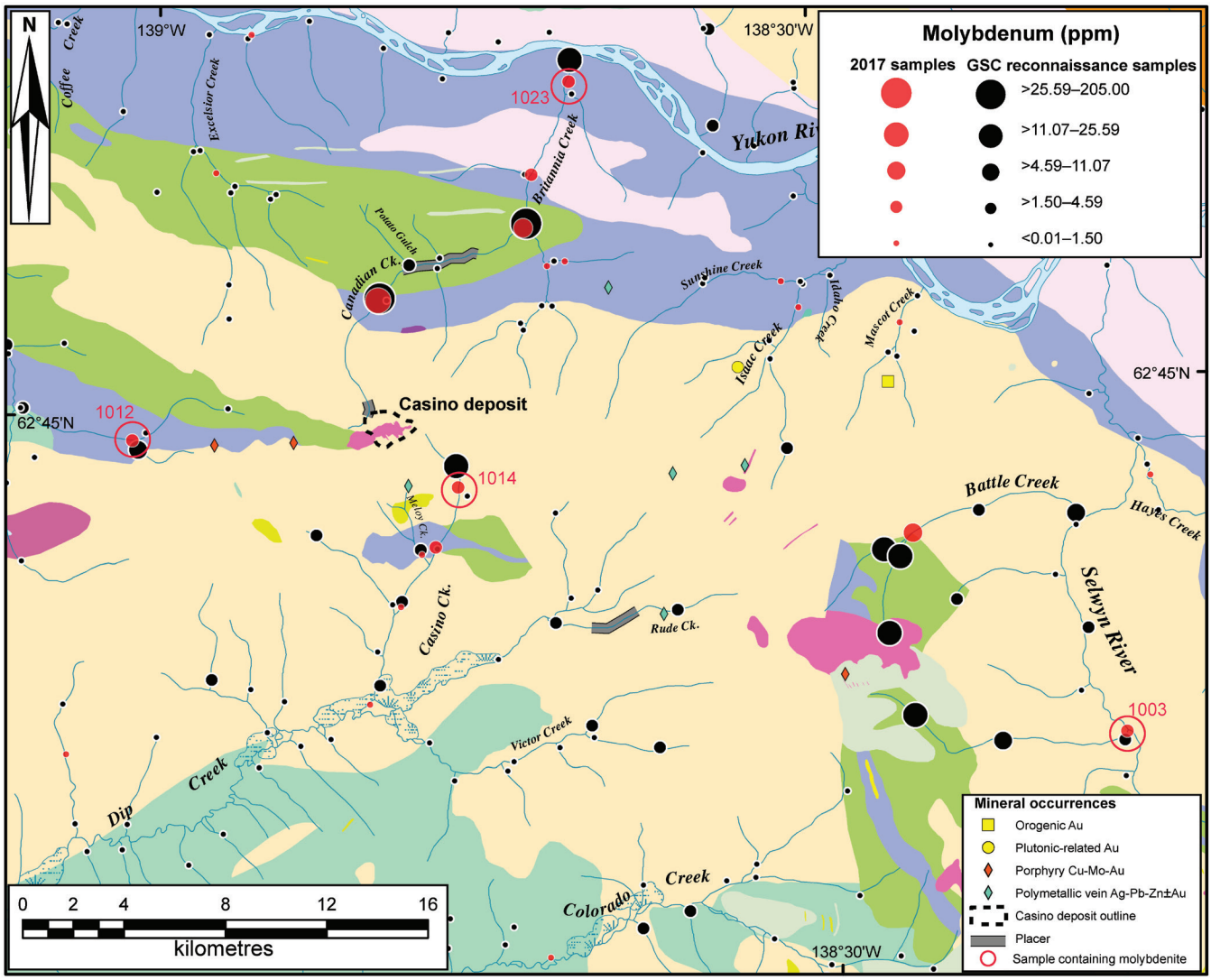

Figure 6. Location of stream-sediment samples containing molybdenite grains in heavy mineral concentrates (red circles and red sample numbers) and molybdenum concentrations, for the less than 0.177 mm fraction of stream-sediment samples collected during 2017 (this study, red dots, n = 22) and reconnaissance samples reanalyzed in 2011 (black dots, n = 1301; Jackaman, 2011). *See* Figure 2 for bedrock geology legend.

and zircon were recovered from stream sediments (Table 2) but their distribution patterns do not reflect the presence of the Casino deposit.

Stream-sediment geochemistry

Comparison of Au analytical methods

The range of Au values determined by all three analytical methods in 2017 are compared in scatterplots in Figure 8a–c. Note that one extremely high fire assay Au value (4056 ppb in sample 1010) was not included in Figure 8 so that similar scales could be used on all three plots, making visual comparisons easier for readers. Gold concentrations determined by INAA (<2–211 ppb) and fire assay (6–4056 ppb) are higher than those by aqua regia followed by ICP-MS (0.8–23.7 ppb). Fire assay and INAA values are most similar, with the fire assay values being slightly higher.

Spatial patterns

Correlation coefficients for the 2017 data are summarized in Figure 9. Copper displays strong positive correlations with Au, Ag, Bi, Cd, Mn, Mo, Pb, W, and Zn, thus all these elements should be considered as pathfinder elements for porphyry copper mineralization in the area. The 2017 data for Cu, Mo, Au by aqua regia, and Au by fire assay were each plotted with data from the GSC reconnaissance samples

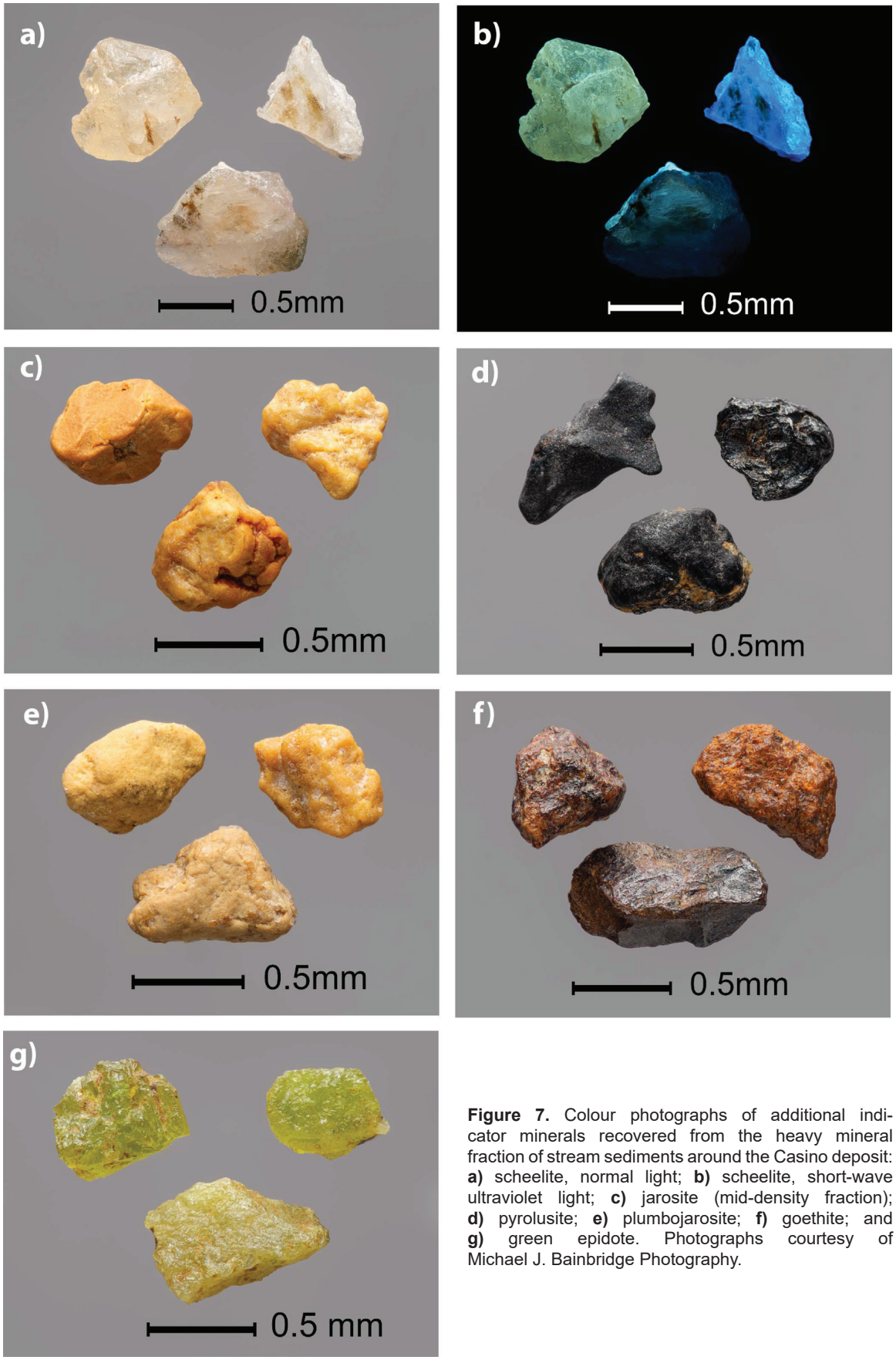

Figure 7. Colour photographs of additional indicator minerals recovered from the heavy mineral fraction of stream sediments around the Casino deposit: **a)** scheelite, normal light; **b)** scheelite, short-wave ultraviolet light; **c)** jarosite (mid-density fraction); **d)** pyrolusite; **e)** plumbojarosite; **f)** goethite; and **g)** green epidote. Photographs courtesy of Michael J. Bainbridge Photography.

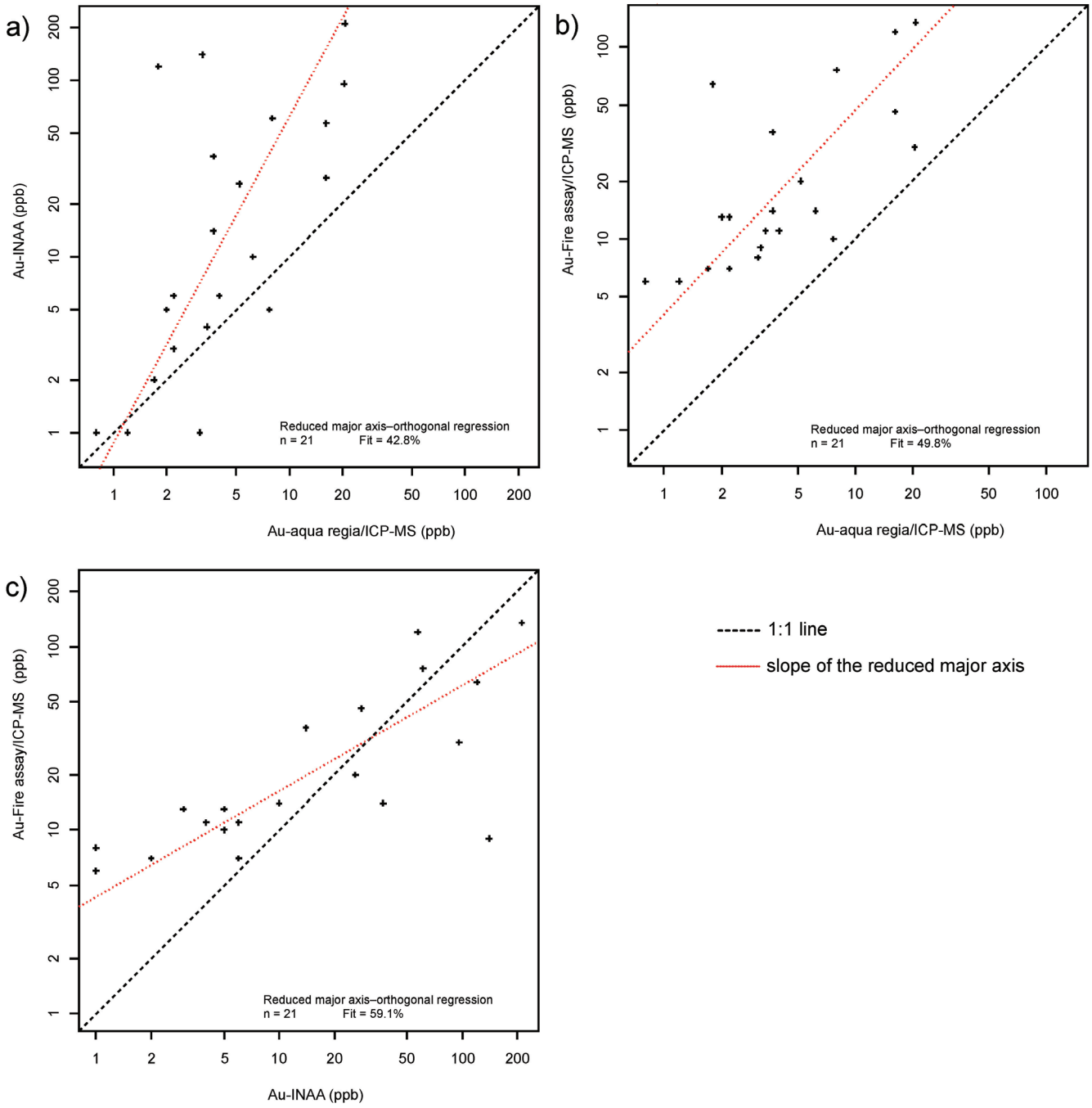

Figure 8. Reduced major-axis plots of Au concentrations in the less than 0.177 mm fraction of 21 stream silt samples determined by three analytical methods in 2017: **a)** instrumental neutron activation analysis (INAA; 30 g sample) versus aqua regia (AR) and inductively coupled plasma mass spectrometry (ICP-MS; 0.5 g sample); **b)** fire assay and ICP-MS (30 g sample) versus AR and ICP-MS (0.5 g sample); and **c)** INAA (30 g sample) versus fire assay and ICP-MS (30 g sample). Data are log transformed.

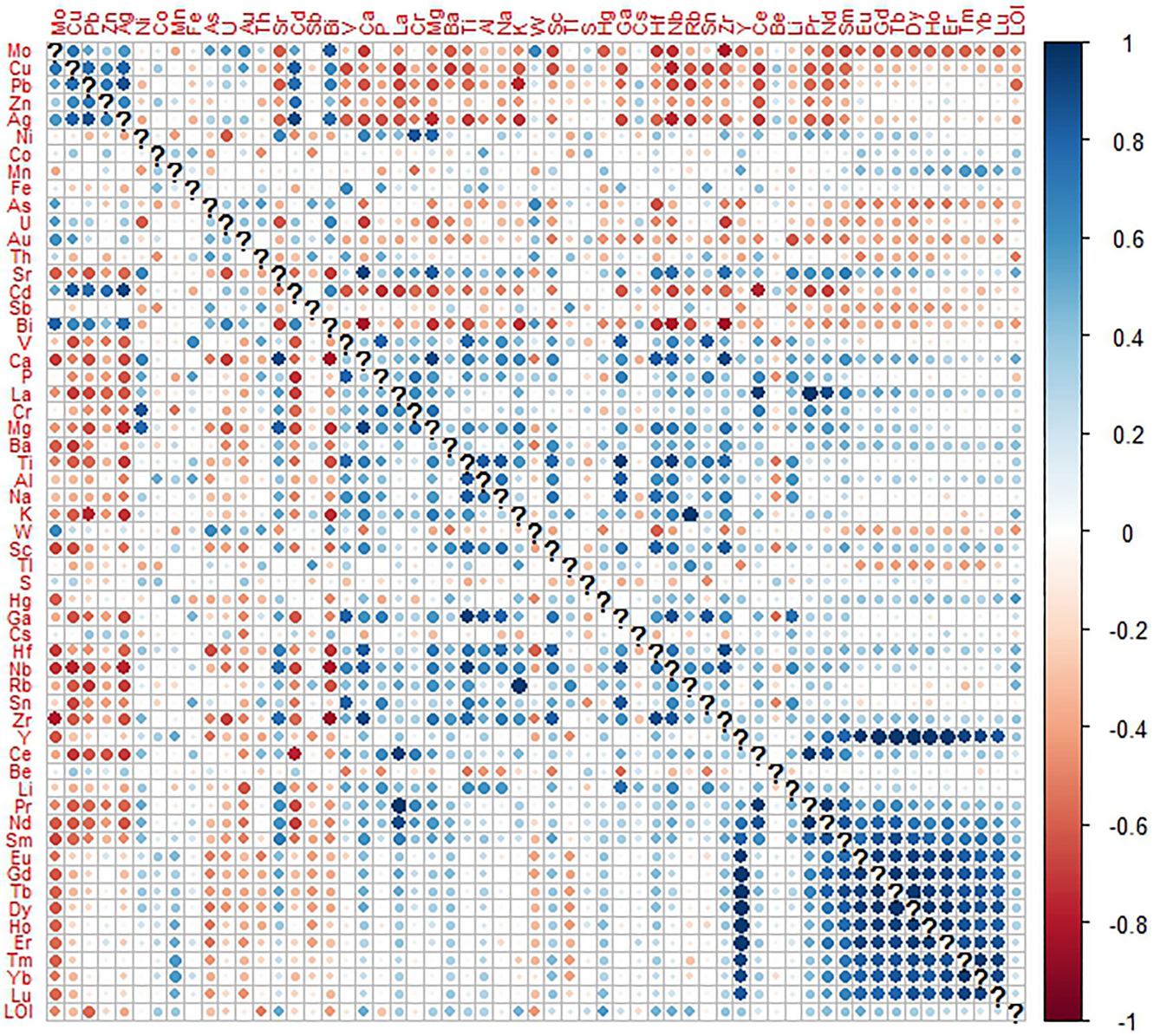

Figure 9. Graphic display using symmetric coordinates to calculate Spearman correlation coefficients between the abundances of elements in 22 stream-silt samples determined by aqua regia and inductively coupled plasma mass spectrometry (ICP-MS) and loss-on-ignition (LOI). The symmetric coordinate procedure is uninfluenced by the closure inherent to geochemical data, that is they are relative and sum to a constant (Garrett et al., 2017; Reimann et al., 2017). Small dots reflect weak correlation and large dots reflect strong correlation. The colour scale indicates the strength of the correlation.

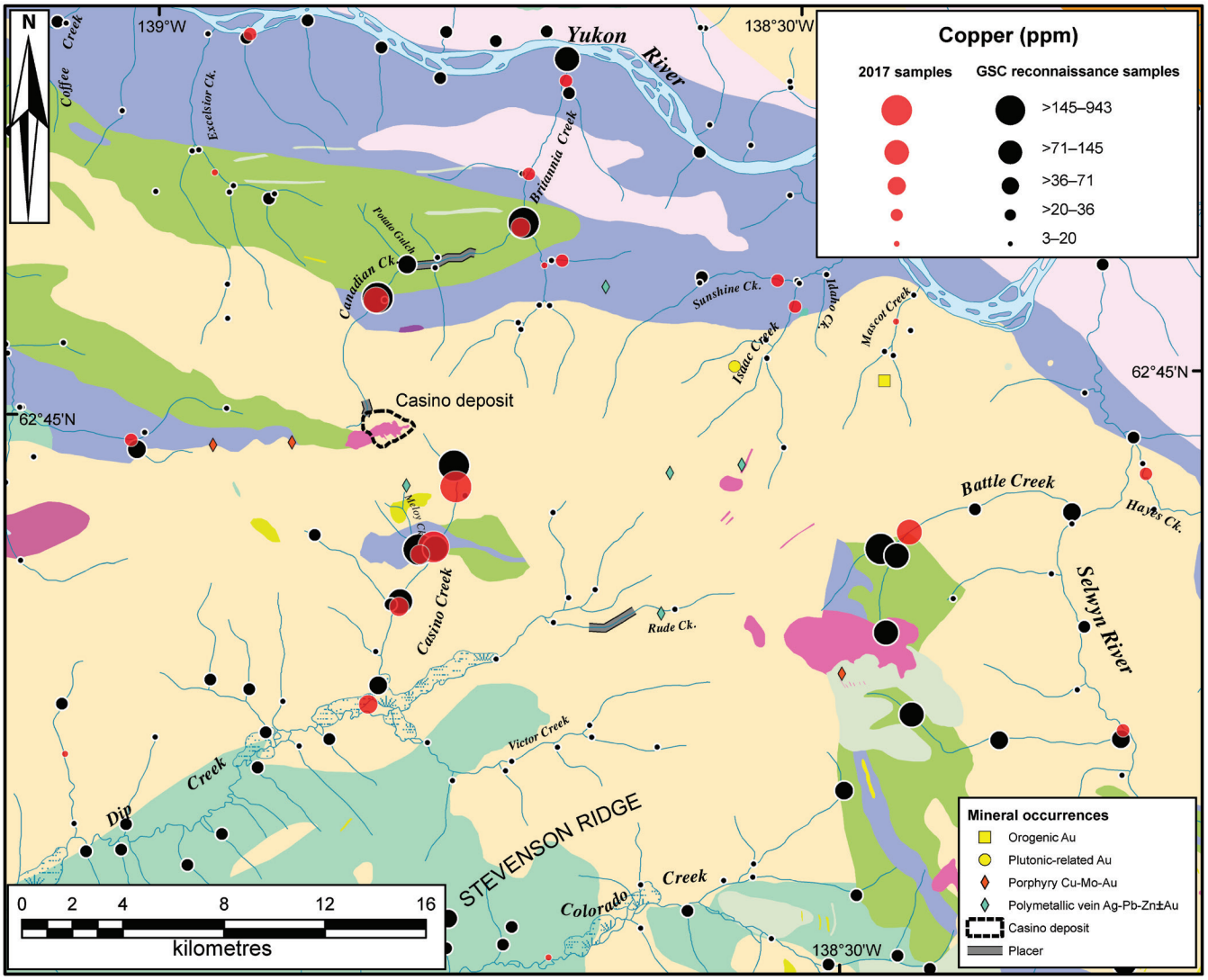

Figure 10. Comparison of copper abundance data for the less than 0.177 mm fraction of stream-sediment samples determined by aqua regia/inductively coupled plasma mass spectrometry in 2017 (this study; red dots, n = 22) and reconnaissance samples reanalyzed in 2011 (black dots, n = 1301; Jackaman, 2011). *See* Figure 2 for bedrock geology legend.

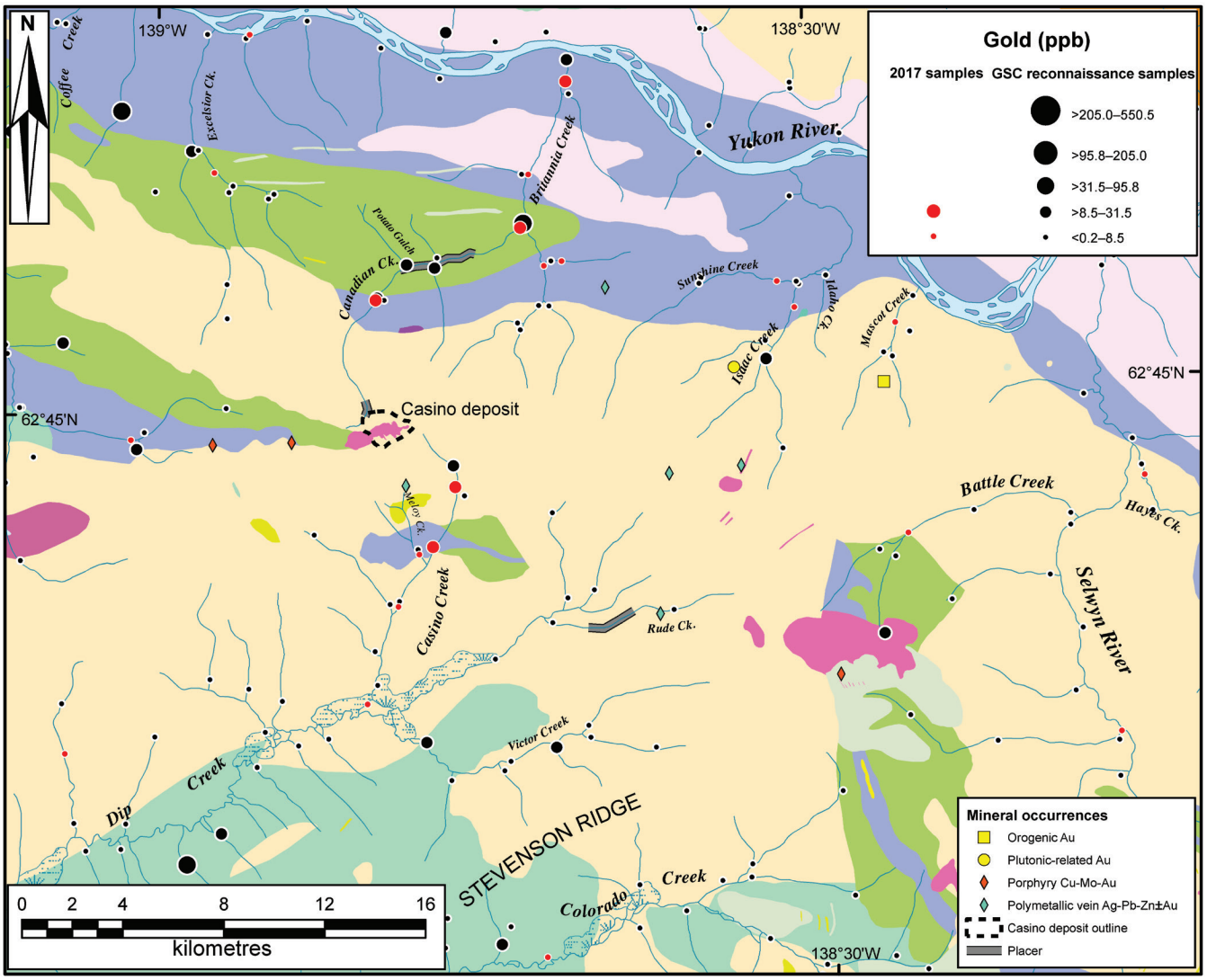

Figure 11. Comparison of gold abundance data for the less than 0.177 mm fraction of stream-sediment samples determined by aqua regia and inductively coupled plasma mass spectrometry (ICP-MS) in 2017 (this study; red dots, n = 22) and reconnaissance samples re-analyzed in 2011 (black dots, n = 1301; Jackaman, 2011). *See* Figure 2 for bedrock geology legend.

collected in NTS map areas 115J and 115K in 1986. Figures 6, 10, and 11 plot aqua regia and ICP-MS data for the 2017 samples (red dots) and the earlier, reanalyzed reconnaissance samples (black dots; Jackaman, 2011). Figure 12 is a plot of Au determined by fire assay and ICP-MS during this study (red dots) and fire assay preconcentration followed by INAA of the doré bead in 1986 (black dots; Geological Survey of Canada, 1987). Proportional dot sizes for both data sets were determined using a subset of the reconnaissance data set for the NTS map areas, not just the samples that plot in the study area, using the Jenks natural breaks method (Howard et al., 2008) in ArcGIS.

Copper concentrations in stream silt samples (Fig. 10) are highest in the two creeks draining the Casino deposit (Casino and Canadian) and in Battle Creek, which drains the Cockfield occurrence. The 2017 values are similar to the 1986 reconnaissance samples at nearby locations even though these older samples were collected 30 years earlier.

Gold (aqua regia) concentrations in 2017 stream silts are moderate (8–31 ppb) in the Casino, Canadian, and Britannia creeks and low (<8 ppb) elsewhere (Fig. 11). Gold (aqua regia) concentrations in the 1986 reconnaissance samples are similar to the 2017 values in Casino Creek but are slightly higher than the 2017 samples in Canadian Creek (maximum 69 ppb). Figure 12 shows that Au (fire assay) values are similar between the 1986 and 2017 samples, except for at sites 1010 (Casino Creek), and 1025 and 1026 (Canadian Creek), where Au values in 2017 samples are considerably higher.

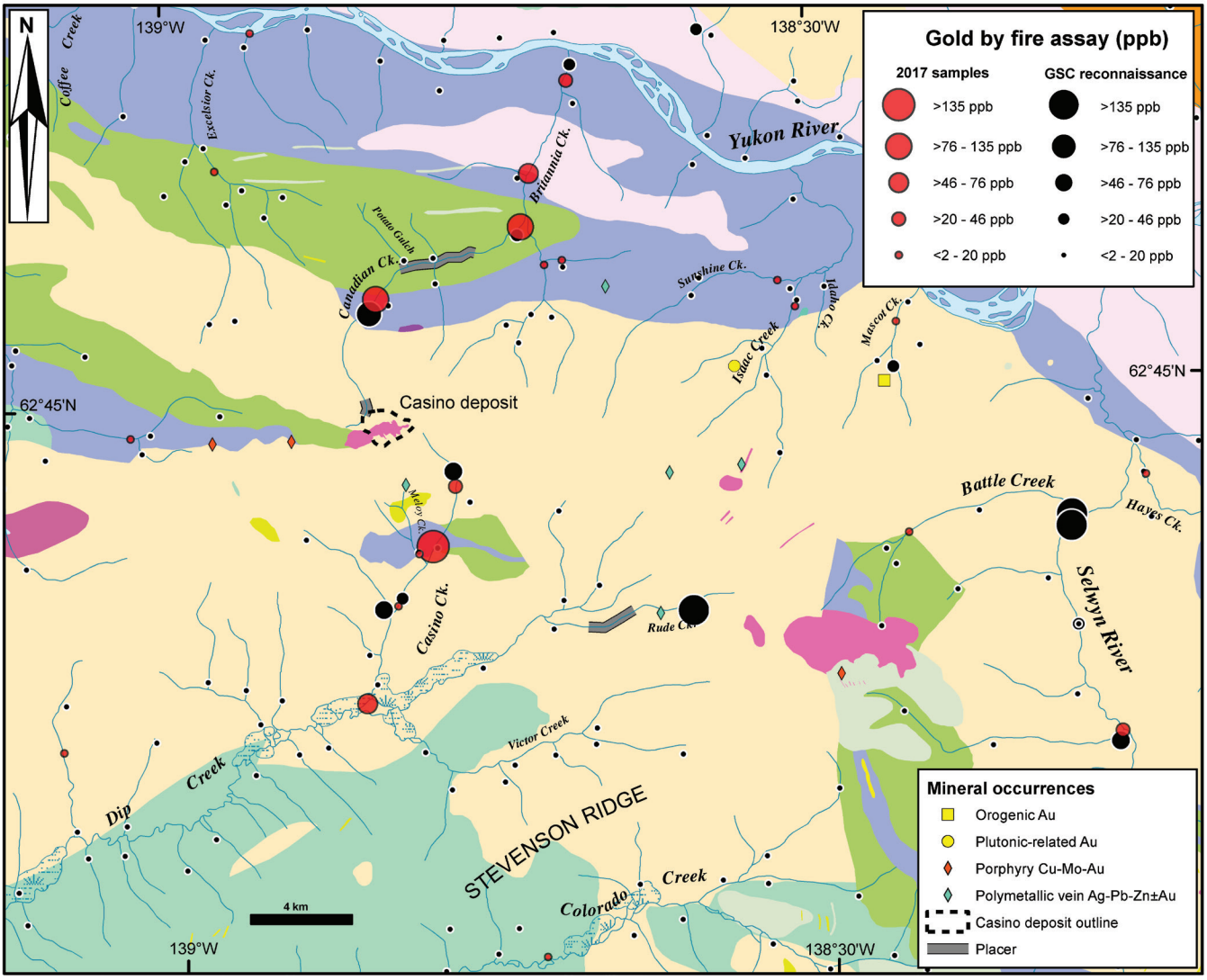

Figure 12. Comparison of gold abundance data for the less than 0.177 mm fraction of stream-sediment samples determined by fire assay in 2017 (this study; red dots, n = 22) and reconnaissance samples (black dots, n = 1301; Geological Survey of Canada (1987)). *See* Figure 2 for bedrock geology legend.

Molybdenum values (Fig. 6) are highest downstream of the Casino deposit in Canadian Creek and downstream of the Cockfield occurrence in Battle Creek. In all cases, the 2017 values are lower than the 1986 reconnaissance samples but show the same general trends in concentration. The lower values in 2017 may be related to differences in the digestion protocols used in 1986 (3:1 HNO_3:HCl) and 2017 (1:1 HNO_3:HCl).

Although not shown on maps, the highest concentrations of Ag, Bi, Te, and W (aqua regia) occur in similar locations to the highest Au (fire assay, INAA) values, that is in Casino and Canadian creeks, and downstream from the Cockfield occurrence. Similar to Cu, the highest concentrations of Cd, Pb, and Zn in stream sediments are on the south side of the Casino deposit in Casino and Meloy creeks. Antimony content is greatest in samples from Meloy, Canadian, and Sunshine creeks.

Portable XRF

The concentrations of elements determined using pXRF on dried, unsieved splits of the stream-sediment samples display similar trends to the less than 0.177 mm aqua regia and ICP-MS data for As, Cu, Mn, Mo, Zn (Fig. 13), and S, and less than 0.177 mm INAA data for Fe. Concentrations for other elements determined by pXRF were too low to be detected, not readily detected by pXRF, or much lower than the values determined by aqua regia and ICP-MS.

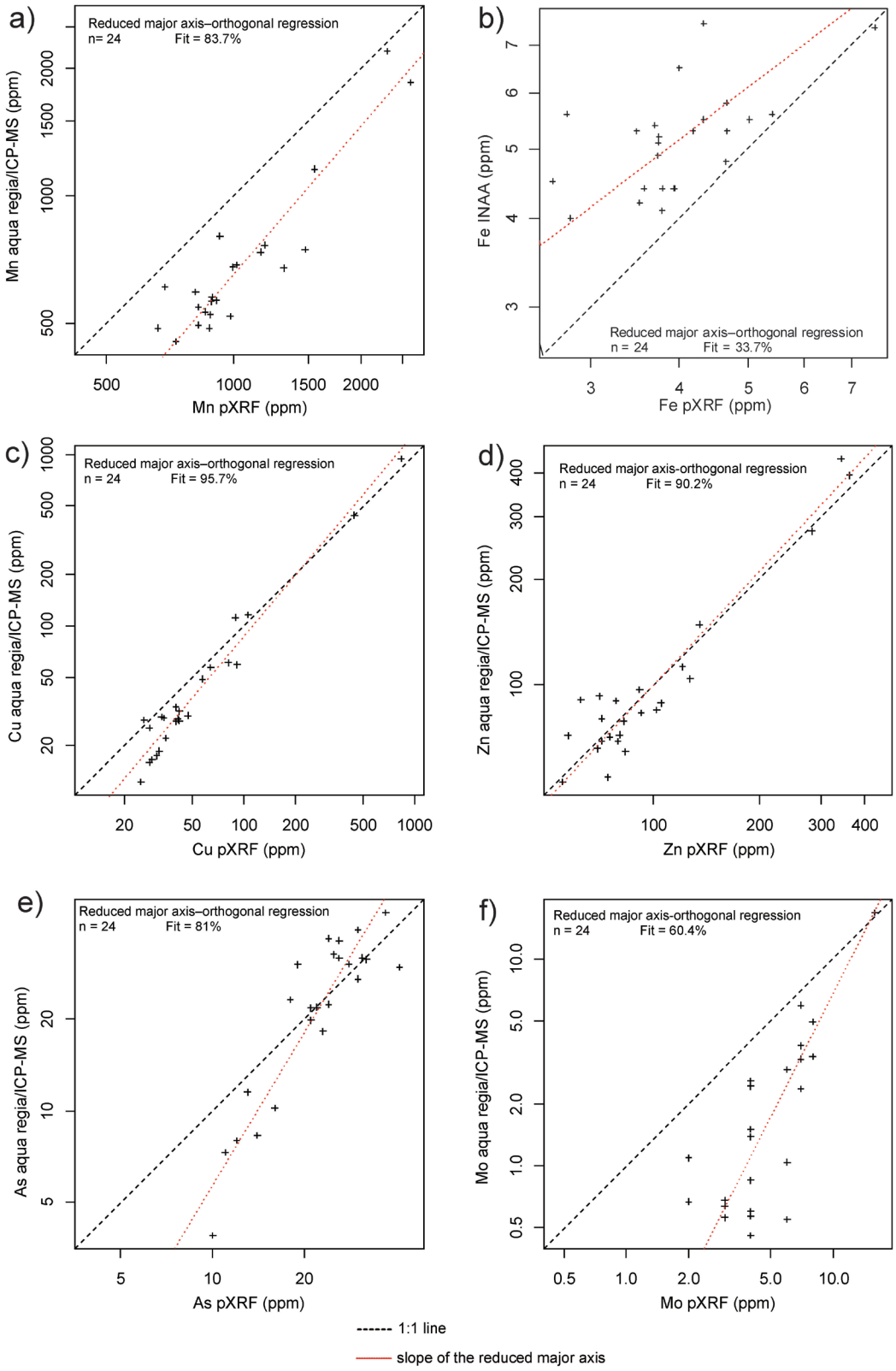

Figure 13. Reduced major-axis plots comparing log-transformed element concentrations in stream-sediment samples determined by aqua regia and inductively coupled plasma–mass spectrometry (ICP-MS) or instrumental neutron activation analysis (INAA) of the less than 0.177 mm fraction and portable X-ray fluorescence (pXRF) of dry, unsieved stream silt: **a)** Mn; **b)** Fe; **c)** Cu; **d)** Zn; **e)** As; and **f)** Mo.

Water geochemistry

Comparison of surface and groundwater

Ground- and streamwater pH values for samples collected in the area around the Casino deposit range from 6.7 to 8.3, values that are typical to slightly alkaline for groundwater and stream water in crystalline rock systems (Leybourne et al., 2006). Groundwater and stream water from the Casino study area are dominantly $CaHCO_3$ to $CaSO_4$ type (Fig. 14).

The Casino groundwater samples typically have higher salinities, with total dissolved solids (TDS) ranging from 74 to 1320 mg/L, whereas TDS in streamwater samples range from 98 to 654 mg/L (Fig. 15). Groundwater salinities are highest proximal to the Casino deposit, whereas streamwater salinities are highest in creeks draining to the north of the deposit. Stream water and groundwater are dominated by Ca (and Mg) as the major cations, with only four samples showing slightly elevated Na concentrations (14–20 mg/L; Fig. 15). All waters have low Cl (<1 mg/L) and F (<1 mg/L) concentrations, and anions are dominated by HCO_3 and, particularly in the groundwater samples close to the Casino deposit, by SO_4 (up to 800 mg/L SO_4; Fig. 15). Thus, Ca, Mg, HCO_3, and SO_4 show relatively strong correlations with TDS (r = 0.985, 0.893, 0.502, and 0.963, respectively).

Selected trace-element concentrations in groundwater and surface water samples have been plotted against dissolved SO_4 (Fig. 16) because oxidation of sulfide minerals is a primary mechanism for increasing SO_4 in shallow waters in crystalline terranes; there are no chemical (evaporite) sediments in the catchment. Stream waters around the Casino deposit have low sulfate concentrations (55 to 84 mg/L) except for sample 1014, which is adjacent to the deposit (105 mg/L). The highest sulfate concentrations (>100 mg/L) in the stream water in the study area occur in Britannia and other creeks to the north of the Casino deposit. Generally, samples with the highest sulfate concentrations have the highest metal and metalloid concentrations. Iron concentrations in most waters in the study area are low (<0.1 mg/L), typical of stream water exposed to atmospheric oxygen. In contrast, the more saline, higher sulfate groundwater has elevated Fe and Mn concentrations (<100 and 10 000 mg/L, respectively; Fig. 16). Groundwater with elevated Fe and Mn also has elevated Cu, Mo, As, Re, B, U, and Zn concentrations (Fig. 16), with values up to greater than 1000, 25.2, 17, 0.71, 11.7, 39.6, and 354 µg/L, respectively.

Spatial patterns

Values for pH change only slightly between samples closest to mineralization (pH = 7.21) and samples farther downstream in Casino Creek (pH = 7.9). Water samples from Casino Creek collected up to 14 km downstream of the Casino deposit have elevated concentrations of Mo, Cu (Fig. 17, 18, respectively), Zn, Pb, Cd, Co, and Re compared to other samples in the study area. Site 1002, downstream from the Cockfield occurrence, has moderately elevated Cd and Cu concentrations and the highest Mo concentration (2.9 ppb) of all the streamwater samples in this study.

DISCUSSION

Indicator minerals

Studies of porphyry copper indicator minerals in glaciated terrain have reported two groups of indicator minerals (Plouffe and Ferbey, 2017). The first group includes minerals that can be directly linked to porphyry mineralization based on their spatial distribution and abundance in bedrock or surficial sediments; the second group includes minerals for which mineral chemistry must be used to establish the link to porphyry copper mineralization. Group 1 indicator minerals recovered from stream-sediment samples around the Casino deposit (Casino, Meloy, Canadian creeks) include chalcopyrite, pyrite, gold, molybdenite, sphalerite, jarosite, and goethite. The distribution of these minerals in local stream sediments in this study is a direct indication of the presence of porphyry Cu mineralization or peripheral Pb-Zn-Ag veins.

Well rounded molybdenite grains (not flakes; Fig. 3d) were recovered from stream sediments downstream of the Casino deposit as well as two porphyry copper occurrences in the area. Molybdenite was observed by Bostock (1959) in the upper Canadian Creek placer occurrence on the west flank of the deposit. Its presence in local creeks is unexpected because molybdenite is soft (hardness = 1) and thus is not expected to survive fluvial transport. In the glaciated terrain of eastern Canada, molybdenite was only recovered from till and stream sediment samples that directly overlie (i.e. <1 km of transport) the intrusion-hosted Sisson W-Mo deposit (McClenaghan et al., 2017) and not in samples down-ice or downstream.

Local stream sediments also contain potential Group 2 minerals: epidote, tourmaline, scheelite, zircon, barite, and magnetite. Studies of tourmaline chemistry are ongoing (Beckett-Brown, 2019, this volume) and results to date indicate that a combination of physical characteristics (lack of inclusions, dark brown–black colour) and chemical characteristics (oxy-dravite to povondraite trend, high concentrations of Sr, low concentrations of Zn and Pb) of the tourmaline grains can distinguish between porphyry-derived and background tourmaline in stream sediments. Future studies comparing mineral chemistry of tourmaline, magnetite, epidote, zircon, and scheelite in the Casino deposit to those recovered from local stream sediments may provide additional insights into the bedrock source(s) of these mineral grains (e.g. Baksheev et al., 2012; Cooke et al., 2014, 2017; Bouzari et al., 2016; Kobylinski et al., 2017, 2018; Wilkinson et al., 2017; Poulin et al., 2018; Plouffe et al., 2019, this volume).

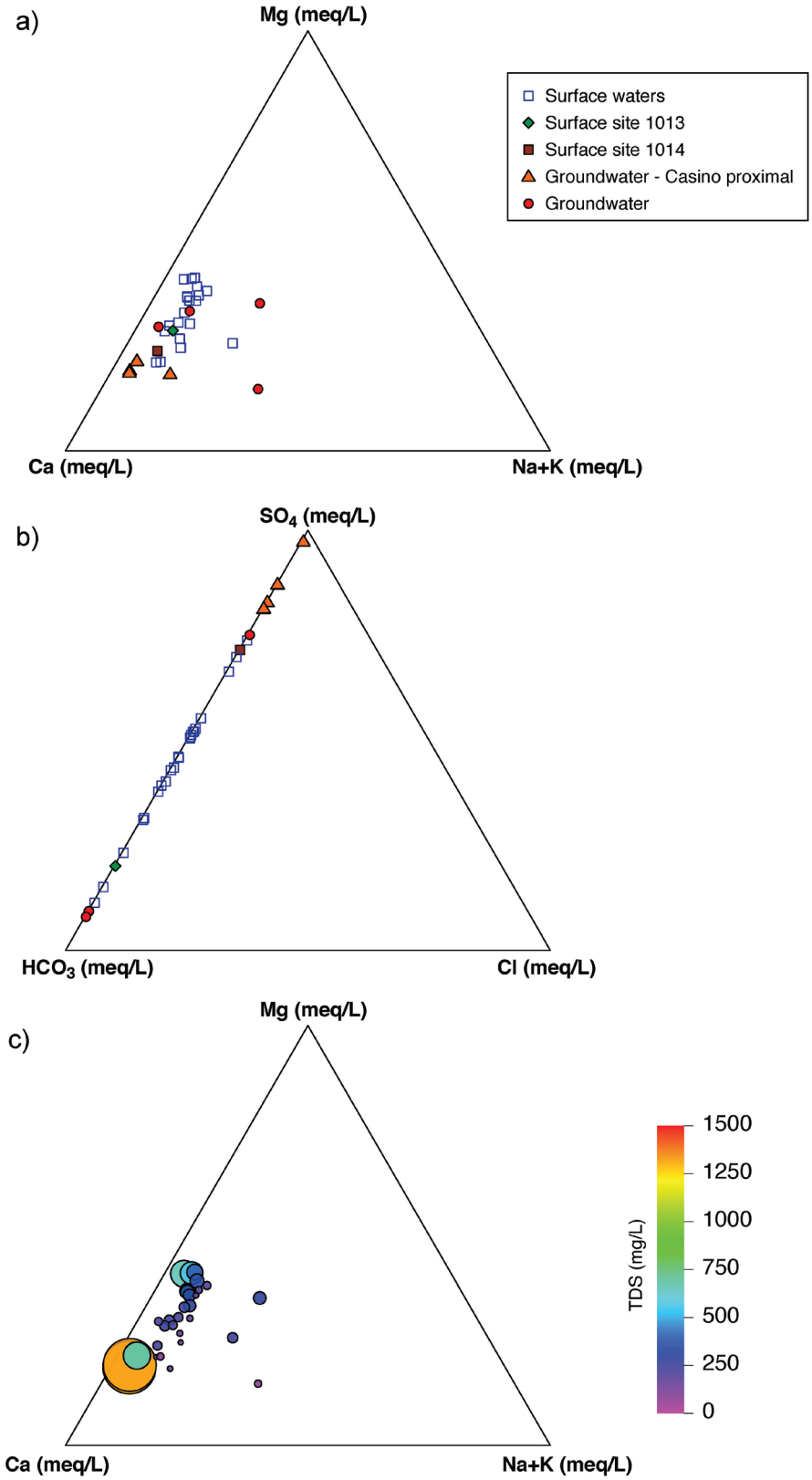

Figure 14. Modified piper plots of surface and groundwaters in the Casino deposit area: **a)** cations; **b)** anions; **c)** total dissolved solids (TDS). Waters closest to the Casino deposit have proportionally higher SO_4 and Ca concentrations and the highest TDS values (n = 31 surface water plus groundwater). Streamwater samples that are closest to the Casino deposit (1013 and 1014) are plotted as unique symbols.

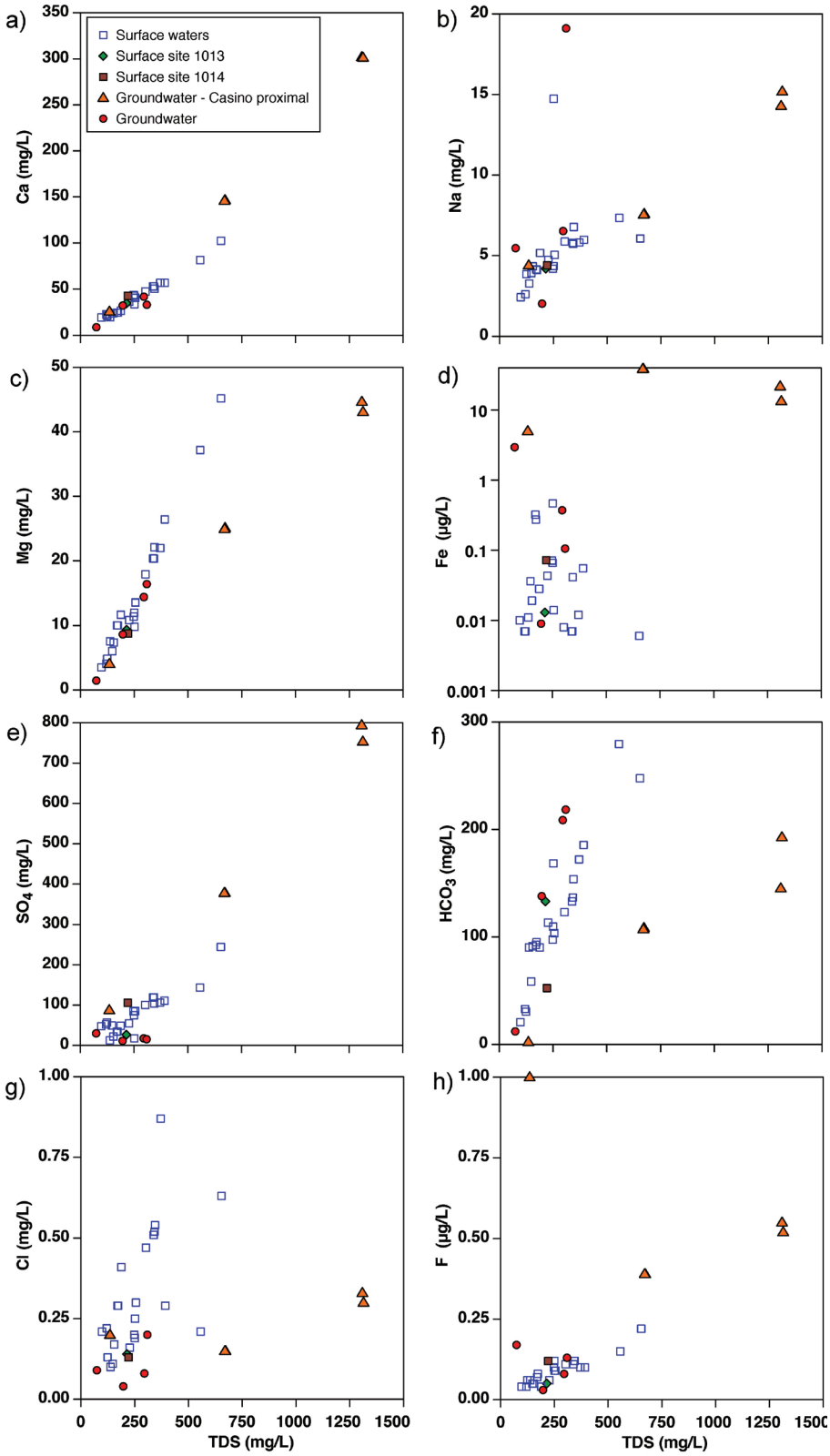

Figure 15. Plots of major ion, Fe and F concentrations versus total dissolved solids (TDS) for surface and groundwaters in the Casino deposit area (n = 31 surface water plus groundwater): **a)** Ca; **b)** Na; **c)** Mg; **d)** Fe; **e)** SO_4; **f)** HCO_3; **g)** Cl; and **h)** F. Streamwater samples that are closest to the Casino deposit (1013 and 1014) are plotted as unique symbols.

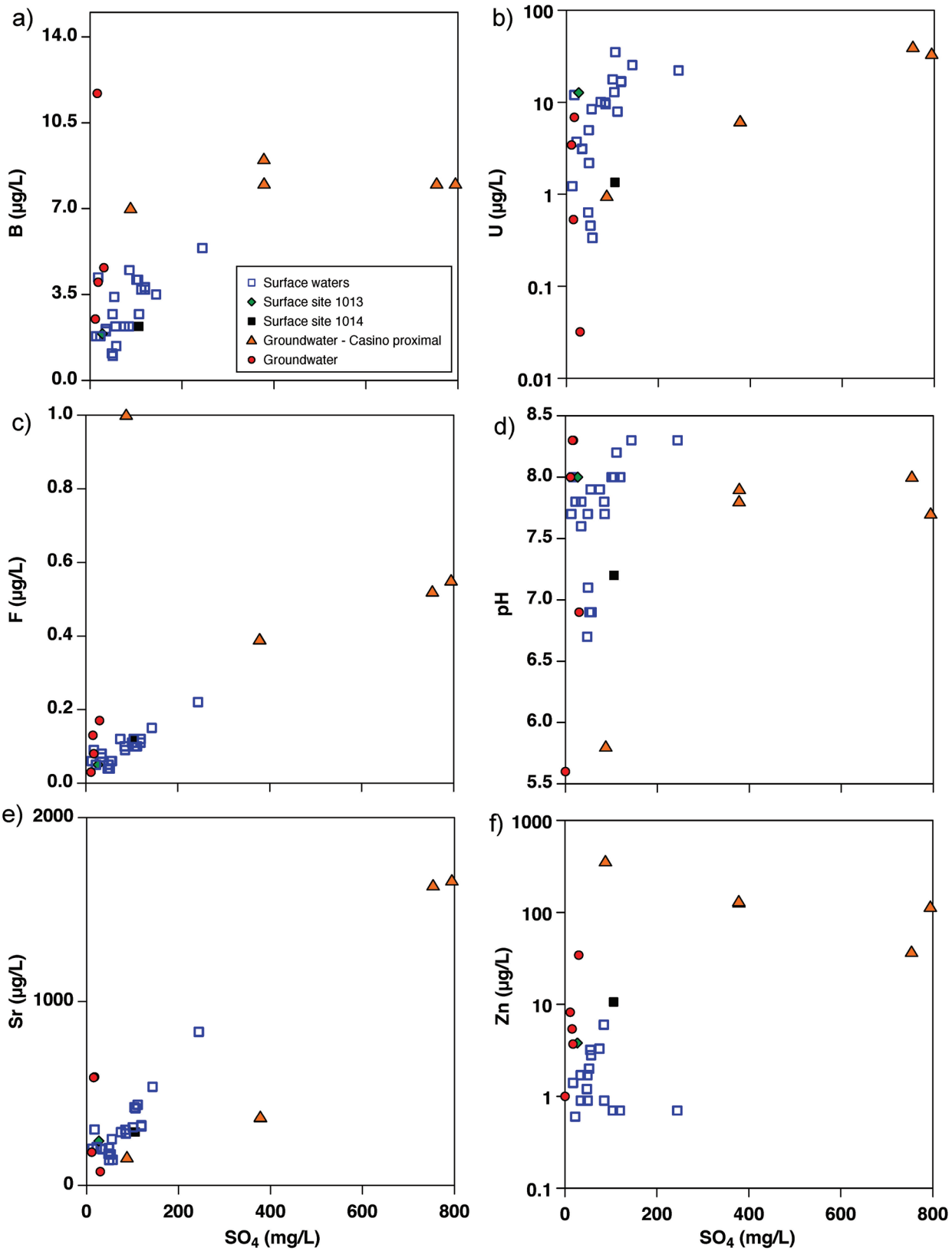

Figure 16. Plots of trace-element concentrations and pH versus SO_4 concentration for surface and groundwaters in the Casino deposit area (n = 31 surface water plus groundwater): **a)** B; **b)** U; **c)** F; **d)** pH; **e)** Sr; and **f)** Zn. Streamwater samples that are closest to the Casino deposit (1013 and 1014) are plotted as unique symbols.

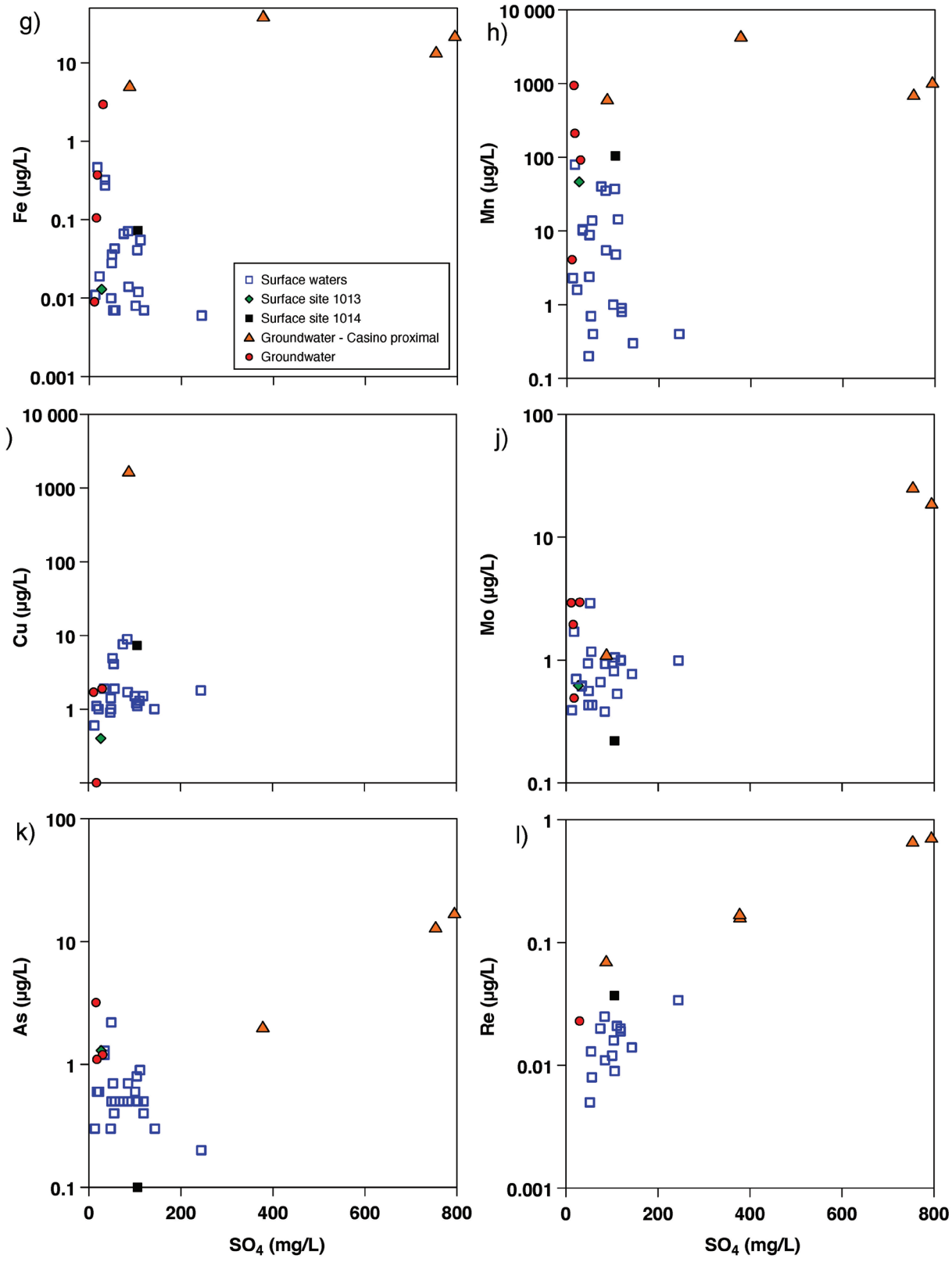

Figure 16 (cont.). Plots of trace-element concentrations and pH versus SO_4 concentration for surface and groundwaters in the Casino deposit area (n = 31 surface water plus groundwater): **g)** Fe; **h)** Mn; **i)** Cu; **j)** Mo; **k)** As; and **l)** Re. Streamwater samples that are closest to the Casino deposit (1013 and 1014) are plotted as unique symbols.

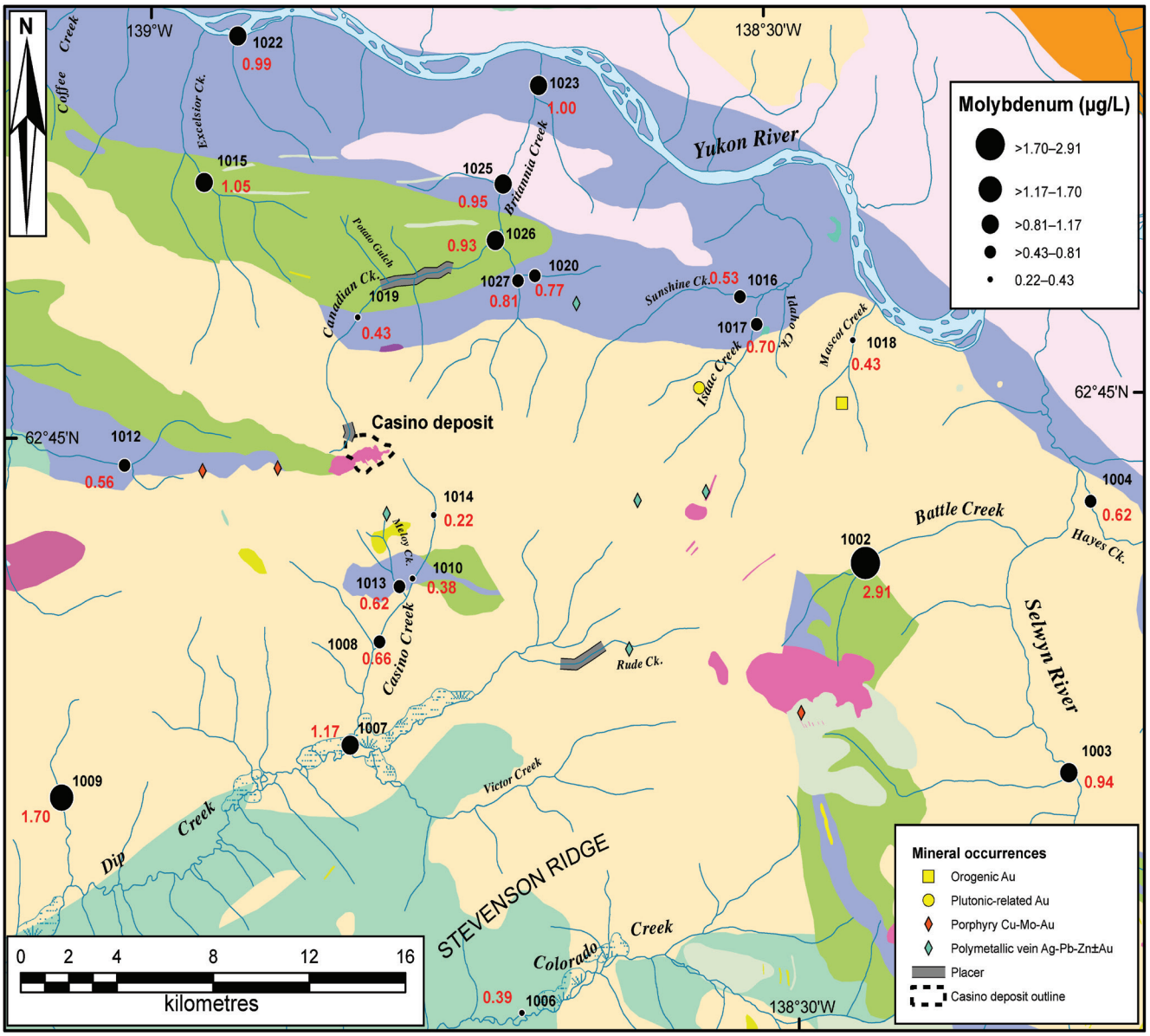

Figure 17. Concentrations of Mo in streamwater samples (n = 22) collected in 2017 in the Casino deposit area. Sample numbers are labelled in black; values are reported in red. *See* Figure 2 for bedrock geology legend.

Gold grains

Numerous 25 to 100 µm gold grains were recovered from bedrock samples examined in this study; this is similar to the gold grain-size range (50–70 µm) reported by Huss et al. (2013) for the hypogene zone, but Chapman et al. (2014) reported a broader range (5–1000 µm). The largest dimension of approximately 80% of the gold grains in stream-sediment samples from creeks immediately draining the Casino deposit (Table 3) is similar (25–200 µm) to that for bedrock samples. Not surprisingly, gold grain shapes in local creeks around Casino are a combination of modified and reshaped, reflecting fluvial transport.

Based on gold grain alloy compositions and mineral inclusion assemblages, Chapman et al. (2014, 2018) concluded that gold in the Canadian Creek placer occurrence downstream of Potato Gulch was a mixture of grains derived from the Casino deposit and from shallow epithermal mineralization. The chemistry and inclusion compositions of gold grains in GSC samples are under investigation and will be compared to the results of Chapman et al. (2014, 2018) in future work.

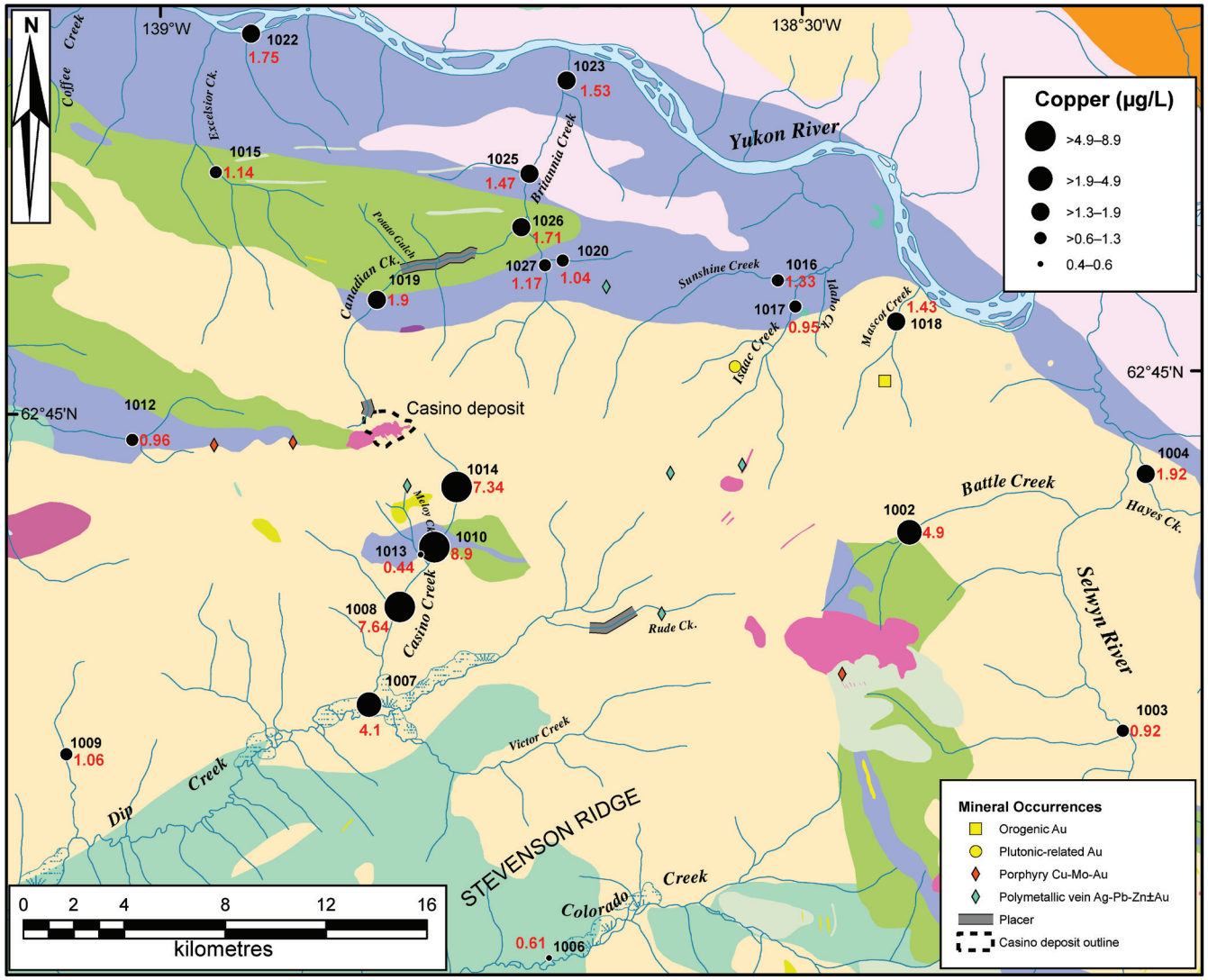

Figure 18. Concentrations of Cu in streamwater samples collected in 2017 in the Casino deposit area. Samples numbers are labelled in black; values are reported in red. *See* Figure 2 for bedrock geology legend.

Comparison of local creeks draining the deposit

Abundances for selected indicator minerals in samples from the creeks that drain the Casino deposit (Casino, Meloy, Canadian, Britannia) are listed in Table 4. Thresholds between background and anomalous indicator mineral abundances were estimated using distal samples 1006 and 1009, which contain very few indicator minerals and have low metals values in stream sediments. This estimation of background based on just two samples is not optimal and could be improved if additional heavy-mineral sampling was conducted in the area.

Abundances of gold, chalcopyrite, pyrite, molybdenite, sphalerite, jarosite, goethite, and scheelite are greater than the values reported for samples 1006 and 1009. Meloy Creek, which drains the Bomber Pb-Zn-Ag vein area, displays a similar suite of indicator minerals without gold and with the addition pyrolusite and plumbojarosite. The presence of pyrolusite in this sample was not unexpected because black manganese coatings were observed on stream cobbles and pebbles at this site. Pyrolusite and plumbojarosite likely formed from the weathering of the Pb-Zn-Ag veins. A pipe discharging water from the Bomber vein adit into the headwaters of Meloy Creek may have contributed to the formation of pyrolusite grains or pyrolusite coatings on other mineral grains in the stream bed at this location.

Table 4. Abundances of selected indicator minerals and trace elements in stream sediments and stream water in samples from the four creeks draining the Casino deposit: Casino, Meloy, Canadian, and Britannia. Samples are listed in order of increasing distance downstream from the deposit. Thresholds for elements in stream sediments are the upper bounds of background variability and were calculated following log transformation of the Yukon-Tanana subset of the 1986 Geological Survey of Canada reconnaissance data (n = 1301; *see* McCurdy et al. (2019) for additional explanation). Background abundances of indicator minerals in stream sediment and elements in water were defined using samples 1006 and 1009. Values greater than the background threshold are highlighted in a colour unique for those minerals that have a direct relationship to an element(s) (e.g. gold grains and Au in ppb). Mineral counts are normalized to 10 kg sample mass and reported for the 0.25 to 0.5 mm >3.2 specific gravity fraction unless otherwise indicated.

Heavy minerals in stream sediment (0.25–05 mm, >3.2 SG)														
Sample site	**Creek**	**Distance down stream from deposit (km)**	**Gold grains**	**Chalco**	**Moly**	**Sphal**	**Plumbo**	**Scheel**	**Jaro SG 2.8–3.2**	**Pyrol**	**Tur SG 2.8–3.2**			
threshold**			1	0	0	0	0	1	45	0	30			
1014	Casino	2.5	1	0	1	9	0	0	132	0	0			
1013	Meloy	3*	0	4	0	11	86	2	36	2518	0			
1019	Canadian	3	28	7	0	1	0	23	31	0	0			
1010	Casino	6	8	0	0	0	0	37	183	0	11			
1008	Casino	9	21	2	0	0	0	4	291	0	4			
1026	Canadian	10	6	2	0	0	0	2	1231	0	62			
1025	Britannia	12.5	19	0	0	0	0	2	1327	0	88			
1007	Casino	13.5	44	0	0	0	0	40	0	0	0			
1023	Britannia	16.5	2	1	1	0	0	0	183	0	0			
Chalco: chalcopyrite; Moly: molybdenite; Sphal: sphalerite; Plumbo: plumbojarosite; Scheel: scheelite; Jaro: jarosite; Pyrol: pyrolusite; Tur: tourmaline; SG: specific gravity														
Stream sediment (<0.177 mm)														
Sample site	**Creek**	**Distance down stream from deposit (km)**	**Au Fire (ppb)**	**Au AR (ppb)**	**Au INAA (ppb)**	**Cu AR (ppm)**	**Mo AR (ppm)**	**Ag AR (ppb)**	**Pb AR (ppm)**	**Zn AR (ppm)**	**Cd AR (ppm)**	**Sb AR (ppm)**	**W INAA (ppm)**	**Mn AR (ppm)**
threshold**			134	12	2**	57	3.8	309	18	123	0.5	0.9	2**	746**
1014	Casino	2.5	46	16	28	943	3.8	441	50	394	3.1	1.3	4	1850
1013	Meloy	3*	11	4	6	57	1.1	1917	568	439	4.8	5.7	2	2194
1019	Canadian	3	120	16	57	115	16.8	412	20	148	1.6	1.4	13	686
1010	Casino	6	4056	24	17	441	3.3	383	37	274	2.0	1.1	6	1154
1008	Casino	9	8	3	<2	59	0.6	139	17	89	0.5	0.5	1	565
1026	Canadian	10	135	21	211	49	5.0	173	15	97	0.7	1.7	11	576
1025	Britannia	12.5	76	8	61	29	2.4	120	12	80	0.4	1.4	4	562
1007	Casino	13.5	64	2	120	61	1.0	201	40	104	0.6	0.9	9	485
1023	Britannia	16.5	30	21	96	32	2.9	116	12	71	0.3	1.2	5	531
Fire: fire assay/inductively coupled plasma mass spectrometry; AR: aqua regia/inductively coupled plasma mass spectrometry INAA: instrumental neutron activation analysis														

Table 4 (cont.). Abundances of selected indicator minerals and trace elements in stream sediments and stream water in samples from the four creeks draining the Casino deposit: Casino, Meloy, Canadian, and Britannia. Samples are listed in order of increasing distance downstream from the deposit. Thresholds for elements in stream sediments are the upper bounds of background variability and were calculated following log transformation of the Yukon-Tanana subset of the 1986 Geological Survey of Canada reconnaissance data (n = 1301; *see* McCurdy et al. (2019) for additional explanation). Background abundances of indicator minerals in stream sediment and elements in water were defined using samples 1006 and 1009. Values greater than the background threshold are highlighted in a colour unique for those minerals that have a direct relationship to an element(s) (e.g. gold grains and Au in ppb). Mineral counts are normalized to 10 kg sample mass and reported for 0.25 to 0.5 mm >3.2 specific gravity fraction unless otherwise indicated.

Stream water

Sample site	Creek	Distance down stream from deposit (km)	Cu (µg/L)	Mo (µg/L)	Ag (µg/L)	Pb (µg/L)	Zn (µg/L)	Cd (µg/L)	Sb (µg/L)	Co (µg/L)	W (µg/L)	Mn (µg/L)	Re (µg/L)	SO_4 (mg/L)
threshold **			1.1	1.70	0.01	0.02	1.4	0.02	0.05	0.15	0.02	79.3	0.005	17.3
1014	Casino	2.5	7.3	0.22	<0.005	0.01	10.6	0.18	0.07	3.86	<0.02	104.1	0.037	105.5
1013	Meloy	3*	0.4	0.62	<0.005	0.15	3.8	0.07	0.19	<0.05	<0.02	46.4	<0.005	26.7
1019	Canadian	3	1.9	0.43	<0.005	<0.01	2.8	0.03	0.21	<0.05	<0.02	0.4	0.008	56.7
1010	Casino	6	8.9	0.38	<0.005	0.01	6.0	0.10	0.11	1.19	<0.02	35.1	0.025	84.3
1008	Casino	9	7.6	0.66	<0.005	0.02	3.3	0.06	0.13	0.48	<0.02	40.1	0.020	74.7
1026	Canadian	10	1.7	0.93	<0.005	0.01	0.9	<0.02	0.32	<0.05	<0.02	5.5	0.011	85.2
1025	Britannia	12.5	1.5	0.95	<0.005	<0.01	<0.5	<0.02	0.24	<0.05	<0.02	1.0	0.012	100.5
1007	Casino	13.5	4.1	1.17	<0.005	0.02	3.2	0.03	0.14	0.07	<0.02	13.8	0.013	54.8
1023	Britannia	16.5	1.5	1.00	<0.005	0.01	0.7	<0.02	0.23	<0.05	<0.02	0.9	0.020	118.9

* Distance downstream from Bomber Pb-Zn-Ag veins
** refer to table caption for an explanation of calculation of thresholds for each sample medium

Comparison with other creeks in the study area

We compare the highest indicator mineral abundances for Casino, Meloy, and Canadian creeks to the highest values reported in stream sediments from other creeks in the study area and to background samples 1006 and 1009 in Table 5. Values greater than the background samples are highlighted using a different colour for each creek. Sediments downstream of the Cockfield (purple) and Zappa (pink) porphyry occurrences display similar suites of anomalous indicator minerals to the those from the creeks draining the Casino deposit (grey) with the exception of gold grains, which are much more abundant in the creeks draining the Casino deposit (Casino and Canadian). The other creeks listed in Table 5 contain noteworthy combinations of gold, sulfide minerals, secondary minerals, scheelite, and tourmaline that could indicate the presence of other types of mineralization.

Sources of minerals in streams

The presence of fresh sulfide minerals in stream sediments from Casino Creek may indicate that the creek is directly eroding less-oxidized parent material related to the Casino deposit and/or peripheral mineralization. Ongoing cryoturbation and downslope gravity movement also contributes weathered and less oxidized material to local creeks. Older gravel deposits along creeks may also be the source of some sulfide minerals.

The minor disturbance from surface exploration activity has likely had minimal impact on the mineralogical and geochemical signatures of the deposit in local creeks, except for at site 1013 on Meloy Creek, where water draining from an old adit into the headwaters of the creek 4 km upstream of the sample site has likely affected the geochemistry of the stream sediment and the water. Former placer mining operations on Canadian Creek may have contributed indicator minerals to Canadian and Britannia creeks.

Stream silt geochemistry

Comparison of local creeks draining the deposit

Abundances for selected trace elements in stream silt samples from the creeks that drain the Casino deposit (Casino, Meloy, Canadian, Britannia) are listed in Table 4. A subset of GSC reconnaissance stream-sediment data (n = 1301) from sites underlain by similar bedrock geology was used to provide a regional context in which to evaluate

Table 5. Comparison of the indicator minerals and elements in stream sediments, silt, and water from the creeks that drain the Casino deposit and other known occurrences in the area. Background thresholds for elements in stream silt are the upper bounds of background variability and were calculated following a log transformation of the Yukon-Tanana subset of the 1986 Geological Survey of Canada reconnaissance data (n = 1301; *see* McCurdy et al. (2019) for additional explanation). Thresholds for indicator minerals and elements in stream water and heavy mineral stream-sediment analyses were defined using samples 1006 and 1009. Anomalous values (greater than the corresponding threshold) are highlighted in a colour unique to each deposit/occurrence.

Sample medium	Mineral/element	Background threshold*	Casino (Casino Creek)	Casino (Canadian Creek)	Bomber veins (Meloy Creek)	Cockfield (Battle + unnamed creek)	Mascot (Mascot Creek)	Buck (Isaac Creek)	Buck (Sunshine Creek)	Marquerite (unnamed Creek)	Zappa (unnamed creek)
Stream HMC	Gold	1	44	29	0	1	3	6	0	14	1
Stream HMC	Chalcopyrite	0	4	7	4	27	1	0	1	0	13
Stream HMC	Molybdenite	0	1	0	0	3	0	0	0	0	3
Stream HMC	Pyrite	0	79	115	11	397	28	3	22	26	2113
Stream HMC	Sphalerite	0	9	1	11	0	0	0	0	0	0
Stream HMC	Bismuthinite	0	0	0	0	1	1	0	0	0	0
Stream HMC	Arsenopyrite	0	0	2	0	3	2	0	0	0	0
Stream HMC	Jarosite	45	291	1231	36	331	0	0	144	0	423
Stream HMC	Plumbojarosite	0	0	0	86	1	0	0	0	0	0
Stream HMC	Pyrolusite	0	0	0	2518	0	0	0	0	0	0
Stream HMC	Goethite	379	18 000	7700	18 000	3311	1724	840	1079	35 000	141
Stream HMC	Hematite	7576	6711	2308	1439	5298	1035	1261	7194	87 000	352
Stream HMC	Scheelite	1	40	23	2	27	4	8	36	11	35
Stream HMC	Tourmaline	30	11	62	0	27	0	0	360	0	0
Stream silt	Au AR (ppb)	12	24	21	4	8	2	4	6	3	5
Stream silt	Au INAA (ppb)		120	211	6	14	5	37	10	4	26
Stream silt	Au Fire (ppb)	134	4056	135	11	36	13	14	14	11	20
Stream silt	Cu (ppm)	57	943	115	57	111	16	22	28	28	29
Stream silt	Mo (ppm)	3.8	3.8	16.8	1.1	6	0.6	0.7	0.6	0.6	2.4
Stream silt	Ag (ppb)	309	441	412	1917	376	121	159	153	123	148
Stream silt	Pb (ppm)	18	50	20	578	25	13	10	13	9	12

Table 5 (cont.). Comparison of the indicator minerals and elements in stream sediments, silt, and water from the creeks that drain the Casino deposit and other known occurrences in the area. Background thresholds for elements in stream silt are the upper bounds of background variability and were calculated following a log transformation of the Yukon-Tanana subset of the 1986 Geological Survey of Canada reconnaissance data (n = 1301; *see* McCurdy et al. (2019) for additional explanation). Thresholds for indicator minerals and elements in stream water and heavy mineral stream-sediment analyses were defined using samples 1006 and 1009. Anomalous values (greater than the corresponding threshold) are highlighted in a colour unique to each deposit/occurrence.

Sample medium	Mineral/element	Background threshold*	Casino (Casino Creek)	Casino (Canadian Creek)	Bomber veins (Meloy Creek)	Cockfield (Battle + unnamed creek)	Mascot (Mascot Creek)	Buck (Isaac Creek)	Buck (Sunshine Creek)	Marquerite (unnamed Creek)	Zappa (unnamed creek)
Stream silt	Zn (ppm)	123	393	148	439	90	83	85	72	69	72
Stream silt	Cd (ppm)	0.5	3.1	4.8	1.6	0.9	0.4	0.6	0.4	0.4	0.5
Stream silt	Bi (ppm)	0.6	0.8	1.2	0.6	1.8	0.2	0.2	0.2	0.2	0.4
Stream silt	As (ppm)	32	31	32	30	45	27	22	32	8	30
Stream silt	Sb (ppm)	0.89	1.25	1.73	5.74	1.02	1.55	1.36	1.96	0.51	1.08
Stream silt	Te (ppm)	0.05	0.08	0.13	<0.02	0.09	0.03	0.03	0.03	<0.02	0.08
Stream silt	W (ppm)	0.6	1.8	2.5	0.2	36.3	0.2	0.2	0.2	0.2	0.7
Stream water	Cu (µg/L)	1.10	7.64	1.90	0.44	4.90	1.43	0.95	1.33	1.04	0.96
Stream water	Mo (pbb)	1.70	1.17	0.93	0.62	2.91	0.43	0.70	0.53	0.77	0.56
Stream water	Pb (µg/L)	0.02	0.02	<0.01	0.15	<0.01	<0.01	<0.01	<0.01	<0.01	<0.01
Stream water	Zn (µg/L)	1.40	10.60	2.80	3.80	2.00	1.70	0.60	<0.05	<0.05	0.90
Stream water	Cd (µg/L)	<0.02	0.18	0.03	0.07	0.06	<0.02	<0.02	<0.02	<0.02	<0.02
Stream water	Co (µg/L)	0.15	3.86	<0.05	<0.05	<0.05	<0.05	<0.05	<0.05	<0.05	<0.05
Stream water	Re (µg/L)	<0.005	0.037	0.71	<0.005	0.005	<0.005	<0.005	<0.005	0.014	<0.005
Stream water	Sb (µg/L)	0.05	0.14	0.32	0.19	0.09	0.27	0.27	0.24	0.06	0.26
Stream water	W (µg/L)	<0.02	<0.02	<0.02	<0.02	<0.02	<0.02	<0.02	<0.02	<0.02	<0.02
Stream water	Bi (µg/L)	<0.02	<0.02	<0.02	<0.02	<0.02	<0.02	<0.02	<0.02	<0.02	<0.02
Stream water	Te (µg/L)	<0.02	<0.02	<0.02	<0.02	<0.02	<0.02	<0.02	<0.02	<0.02	<0.02
Stream water	Mn (µg/L)	79.3	104.1	5.5	46.4	0.7	2.4	1.6	14.3	0.3	8.8
Stream water	SO_4 (mg/L)	17.33	105.54	85.21	26.7	52.59	48.62	22.1	111.05	143.49	49.3

HMC: heavy mineral concentrate; Fire: fire assay/inductively coupled plasma mass spectrometry; AR: aqua regia/inductively coupled plasma mass spectrometry; INAA: instrumental neutron activation analysis
* refer to table caption for an explanation of calculation of thresholds for each sample medium

the 2017 data from the Casino deposit. The fences routine in the R package rgr (Garrett, 2018) was used to estimate the upper and lower bounds of background variability for selected elements in the reconnaissance data, following log transformation of the data. Tukey fences were calculated based on the median and quartiles (25th and 75th percentiles) to obtain the interquartile range of the selected elements. The upper limit of background variability was used as the threshold between background and anomalous populations in the reconnaissance subset (*after* McCurdy et al., 2019) and compared to the highest values reported for each creek sampled in 2017 (Table 4). The elements well above the threshold values are Au, Ag, Bi, Cd, Cu, Mn, Mo, Pb, Sb, Te, W, and Zn and are highlighted with coloured cells in Table 4. The Meloy Creek sample exceeds the threshold for Ag, Cd, Mn, Pb, Sb, and Zn, reflecting its proximity to the Bomber Pb-Zn-Ag veins and water drainage from the old adit into the headwaters.

The pathfinder elements in stream sediments downstream from the Casino deposit are similar to the elements (Cu, Mo, Au) reported in previous stream-sediment surveys around porphyry copper deposits (e.g. Coope, 1973; Huff, 1976; Learned et al., 1985; Britten and Marr, 1995; Richardson, 1995). In our study, Ag, Bi, Cd, Mn, Pb, Sb, Te, W, and Zn are also potential porphyry copper pathfinders in stream silt samples.

Comparison with other creeks in study area

We compare the threshold values to the most abundant indicator minerals and elements reported in other creeks in the study area in Table 5. Anomalous values are highlighted with colours corresponding to each creek. Sediments downstream of the Cockfield occurrence (purple) display similar anomalous element concentrations to those from the creeks draining the Casino deposit (grey) with the exception of Au, which is higher in the creeks draining the Casino deposit. The stream silt geochemical values for the other creeks listed in Table 5 are unremarkable.

Gold in stream sediments

Gold concentrations in 2017 stream-sediment samples are considerably higher in the 30 g aliquots analyzed by fire assay and INAA than in the 0.5 g aliquots analyzed using an aqua regia digestion. The 30 g total (INAA and fire assay) methods show greater contrast between background and anomalous Au concentrations and the Au-rich signature of the Casino deposit (Fig. 12). Aqua regia (0.5 g) values for the 2017 samples may be significantly lower than those of the fire assay and INAA methods because some gold is tied up in undigested minerals such as quartz and/or by the nugget effect because of the smaller aliquot mass (0.5 g versus 30 g). Comparisons of aqua regia Au values to those determined by INAA and fire assay provide indications of amount of Au that might be present as inclusions in mineral phases not dissolved in aqua regia and also not visible in HMCs. This information is useful to the exploration geologist/geochemist. Additional analyses for Au using aqua regia and ICP-MS on 30 g aliquots of the 2017 samples would provide insight into the reasons for the observed differences.

Usefulness of pXRF analysis

A few studies have reported the use of pXRF to characterize the chemical composition of dried, sieved stream-sediment samples in glaciated (Luck and Simandl, 2014; Mackay et al., 2016) and unglaciated (De Almeida et al., 2019) terrains. This study is the first to report data for unsieved stream silt samples and to compare pXRF analyses to aqua regia and ICP-MS as well as INAA analyses of the same samples. The pXRF data display similar trends to commercial laboratory data for Mn, Fe, Cu, Zn, As, Mo (Fig. 13a–f), and S. Greater similarity between element concentrations measured by pXRF and aqua regia or INAA methods would be expected if the samples were dried and sieved prior to pXRF analysis. This study demonstrates that pXRF analyses on unsieved samples can quickly define reasonable differences in concentrations of some elements and can be used to identify geochemical anomalies and guide follow-up sampling while still in the field, saving the project time and money.

Water geochemical patterns

Comparison of creeks

The abundances of selected trace elements in streamwater samples from the creeks that directly drain the Casino deposit are listed in Table 4. Thresholds between background and anomalous streamwater samples were defined using estimated background samples 1006 and 1009. Elements with abundances well above the threshold include Cd, Co, Cu, Zn, and SO_4. The Meloy Creek sample (sample 1013) exceeds the threshold for Cd, Pb, Sb, and SO_4, reflecting its proximity to the Bomber Pb-Zn-Ag veins and the effect of water drainage from the old adit into the headwaters.

We compare the elements with the highest concentrations in the local creeks to those with the highest concentrations in other creeks in the study area in Table 5. Casino and Canadian creek waters (grey) have some of the highest Cu, Mo, Zn, Cd, and Re values for streamwater samples in this study. These high metal values are not unexpected because Archer and Main (1971) reported values of up to 2030 µg/L Cu in stream water from a small creek that drains into upper Casino Creek. Streamwater sample 1013 from Meloy Creek (blue) contains the highest concentration of Pb (0.15 µg/L) reported in this study, as well as high concentrations of

Zn and Cd. This sample is downstream from the Bomber Pb-Zn-Ag veins, and water draining from the old adit into the headwaters of Meloy Creek may have contributed to these high values (Casino Mining Corporation, 2014). Samples 1002 and 1003, from downstream of the Cockfield occurrence (purple), also have high values of Cu, Mo, Zn, and Cd in stream water. Mascot Creek (green) displays elevated concentrations of Cu, Zn, Sb, and SO_4.

Pathfinders in streamwater samples downstream from the Casino deposit reported in this study are similar to those reported in previous streamwater studies of porphyry copper deposits (Cu, Mo, Au, SO_4; e.g. Coope, 1973; Learned et al., 1985; Rebagliati et al., 1995; Taufen, 1997; Eppinger et al., 2012; Mathur et al., 2013). In our study, Cd, Co, Mn, Pb, Re, and Zn are also potential pathfinders for porphyry Cu-Mo-Au deposits in stream water.

Comparison of three sample media

Table 4 compares indicator mineral abundances to selected trace-element concentrations in stream sediments and streamwater in samples from the creeks draining the Casino deposit. Coloured cells are assigned so that a colour is unique to a mineral and its related element(s) (e.g. chalcopyrite and Cu concentrations, sphalerite and Zn concentrations). In general, samples that contain indicator minerals also have elevated concentrations of corresponding elements. This is most obvious between Au concentration and the number of gold grains. All stream-sediment samples in Table 4 contain gold grains, except that from Meloy Creek. Stream sediments contain corresponding anomalous contents of Au (INAA), with very low Au values in samples 1013 and 1008. Trace-element measurements of stream sediment samples will reflect the presence of detrital grains that contain these elements as well as material adsorbed onto the surface of mineral grains on the stream bed.

The Zn content in five stream silt samples is anomalous, but sphalerite was only recovered from three of these samples. In contrast, W content is elevated in three samples, but noteworthy numbers of scheelite grains were detected in seven samples. High Pb content is apparent only in silt sample 1013, which also contains plumbojarosite. Samples 1008, 1023, and 1025 have unremarkable stream silt and water chemistry that would not normally generate further interest, yet the presence of gold grains, chalcopyrite, scheelite, and jarosite in these three samples is worthy of further investigation.

Indicator minerals recovered from local creeks are physical evidence of the presence of mineralization (gold grains, chalcopyrite, molybdenite, sphalerite) or the weathering of the mineralization (jarosite, goethite, plumbojarosite, beudantite). They can be examined with a binocular or scanning electron microscope and chemically analyzed to provide detailed information about the nature of the mineralizing system. They may be present in very low abundances (e.g. 1–2 grains of molybdenite in a 10 kg sample) at sites that do not have a coincident anomalous geochemical signature in stream silt samples.

Indicator mineral information can be especially important for reconnaissance and regional-scale surveys, where the presence of a few indicator grains in broadly spaced samples may indicate that a region is worthy of more detailed sampling. Government and exploration surveys in which detailed follow up is not possible during the same field season would benefit the most from the addition of indicator mineral sampling to stream-sediment sampling programs.

CONCLUSIONS AND IMPLICATIONS FOR EXPLORATION

The purpose of this study is not to redefine the already well-known geochemical signature of the Casino deposit or prove that stream silt geochemistry is well suited to porphyry copper exploration. Instead, the focus is testing the use of indicator minerals as an additional porphyry copper exploration tool for unglaciated terrain. The Casino test site is well suited to this type of study because its geochemical signature in local stream sediments and water is already well known and because the deposit has not yet been mined. The abundances of indicator minerals in stream sediments reported in this paper offer a guide to what might be expected downstream of porphyry Cu-Au deposits in the unglaciated terrain of the Yukon. Indicator minerals provide additional information that silt geochemistry alone cannot.

This study is the first detailed indicator mineral study around a major porphyry copper deposit in unglaciated terrain in Canada. The deposit and/or peripheral mineralization has an obvious indicator mineral signature in stream sediments that consists of, in order of effectiveness, gold>chalcopyrite >molybdenite>sphalerite>jarosite>goethite>pyrite, and is detectable at least 14 km downstream from the deposit in Casino Creek. Similar indicator mineral patterns were detected in creeks downstream of other local porphyry occurrences (i.e. Cockfield and Zappa).

Estimates of threshold values for indicator minerals and streamwater based on only two samples were used to evaluate the data. As more stream sediment heavy mineral sampling is conducted in this region, these thresholds will be refined and improved. Readers are encouraged to read the individual open files that report the raw data for indicator minerals, stream sediments, and stream water and to examine the individual mineral and element distribution maps to fully interpret and compare the data sets.

Stream-sediment sampling is a highly successful geochemical method for porphyry copper exploration globally. Our limited sampling around the Casino deposit confirms this fact. Thirty years after the GSC's reconnaissance-scale survey of the Casino region, the Cu signature in stream sediments around the Casino deposit is almost the same. Few,

if any, stream-sediment studies have ever been repeated 30 years later to demonstrate the similarities or differences in geochemical signatures over time.

FUTURE WORK

Indicator mineral methods are now widely used for precious- and base-metal exploration in the glaciated terrain of Canada. Regional indicator mineral surveys have not been conducted across the unglaciated part of the Yukon and have the potential to provide further insights into the effectiveness of heavy minerals as indicators during porphyry copper and gold exploration in this part of Canada.

Automated SEM-based methods (MLA, QEMSCAN) are useful for detecting indicator minerals in the fine fraction of HMCs (Lehtonen et al., 2015; Layton-Matthews et al., 2017; Lougheed et al., in press). Grain mounts are expensive to prepare and analyze, thus automated SEM-based methods are not yet routinely applied to every heavy mineral sample in government surveys. Future research will include MLA analysis of the less than 0.25 mm heavy and mid-density fractions of bedrock and stream sediments from the Casino deposit to determine the indicator minerals present and how their distribution in creeks is influenced by grain size. Mineral chemistry characterization of gold, tourmaline, scheelite, and magnetite from bedrock and stream sediments is ongoing and will be reported in future publications.

The Cu isotopic compositions of stream water (2017 GSC samples) and groundwater samples collected from drillholes by Western Copper and Gold are being analyzed to investigate the fractionation of copper as a function of sulfide weathering and aqueous transport. Additionally, the isotopic signatures of water will be compared to those of oxidized and fresh mineralized bedrock, and stream sediments. These combined data will provide valuable information regarding the utility of Cu isotopes in aqueous samples as exploration vectors to sulfide mineralization. The Cu isotopic composition of waters may also be useful for indicating if isolated Cu anomalies, such as that measured in water sample 1002 from Battle Creek (Cockfield occurrence; Fig. 18), are related to porphyry copper mineralization. Future investigations of stream silt geochemistry will include aqua regia and ICP-MS analysis of 30 g aliquots to compare the Au content to that determined on 30 g aliquots by INAA and fire assay.

ACKNOWLEDGMENTS

This paper is a contribution to Geological Survey of Canada's Targeted Geoscience Initiative program, through the Porphyry-style Mineral Systems project, Activity P-3.3: Mineralogical markers of fertility porphyry-style systems. We gratefully acknowledge Western Copper and Gold Corporation and the Casino Mining Corporation, and in particular M. Mioska and H. Brown, for providing access, assistance, and knowledge of the deposit. We thank K. Spalding (expediting services), B. Younker (Casino camp manager), A. Turcotte, and L. Turcotte (Casino water sampling) for facilitating GSC fieldwork, and J. Bond, Yukon Geological Survey, for sharing geological information and advice for the Casino area. This paper benefited from thoughtful reviews by D. Arne (Telemark Geosciences), P. Gammon (GSC), and A. Plouffe (GSC), and comments by L. Jackson (GSC–retired).

REFERENCES

Archer, A.R. and Main, C.A., 1971. Casino, Yukon – A geochemical discovery of an unglaciated Arizona-type porphyry; *in* Geochemical Exploration, Proceedings of the 3rd international geochemical exploration symposium, (ed.) R.W. Boyle; Canadian Institute of Mining and Metallurgy, Special Volume 11, p. 67–77.

Arne, D., Mackie, R., and Pennimpede, C., 2018. Catchment analysis of re-analyzed regional stream sediment geochemical data from the Yukon; EXPLORE, Association of Applied Geochemists no. 179, p. 1–13.

Averill, S.A., 2001. The application of heavy indicator mineralogy in mineral exploration with emphasis on base metal indicators in glaciated metamorphic and plutonic terrains; *in* Drift exploration in glaciated terrain, (ed.) M.B. McClenaghan, P.T. Bobrowsky, G.E.M. Hall, and S.J. Cook; Geological Society, London, Special Publication 185, p. 69–81. https://doi.org/10.1144/GSL.SP.2001.185.01.04

Averill, S.A., 2011. Viable indicators in surficial sediments for two major base metal deposit types: Ni-Cu-PGE and porphyry Cu; Geochemistry: Exploration, Environment, Analysis, v. 11, p. 279–291. https://doi.org/10.1144/1467-7873/10-IM-022

Baksheev, I.A., Prokof'ev, V.Y., Zaraisky, G.P., Chitalin, A.F., Yapaskurt, V.O., Nikolaev, Y.N., Tikhomirov, P.L., Nagornaya, E.V., Rogacheva, L.I., Gorelikova, N.V., Kononov, O.V., 2012. Tourmaline as a prospecting guide for the porphyry-style deposits; European Journal of Mineralogy, v. 24, no. 6, p. 957–979. https://doi.org/10.1127/0935-1221/2012/0024-2241

Barkov, A.Y., Martin, R.F., Shi, L., LeBarge, W., and Fedortchouk, Y., 2008. Oscillatory zoning in stanniferous hematite and associated W-and Bi-rich minerals from Canadian Creek, Yukon, Canada; The Canadian Mineralogist, v. 46, no. 1, p. 59–72. https://doi.org/10.3749/canmin.46.1.59

Beckett-Brown, C.E., McDonald, A.M., and McClenaghan, M.B., 2019. Unravelling tourmaline in mineralized porphyry systems: assessment as a valid indicator mineral; *in* Targeted Geoscience Initiative: 2018 report of activities, (ed.) N. Rogers; Geological Survey of Canada, Open File 8549, p. 345–351. https://doi.org/10.4095/313669

Bond, J.D. and Lipovsky, P.S., 2011. Surficial geology, soils and permafrost of the northern Dawson Range; *in* Yukon Exploration and Geology 2010, (ed.) K.E. MacFarlane, L.H. Weston, and C. Relf; Yukon Geological Survey, p. 19–32.

Bond, J.D. and Lipovsky, P.S., 2012a. Surficial geology of Colorado Creek (NTS 115 J/10) Yukon; Yukon Geological Survey, Open File 2012-2, scale 1:50 000.

Bond, J.D. and Lipovsky, P.S., 2012b. Surficial geology Selwyn River (NTS 115 J/09) Yukon; Yukon Geological Survey, Open File 2012-1, scale 1:50 000.

Bond, J.D. and Sanborn, P.T., 2006. Morphology and geochemistry of soils formed on colluviated weathered bedrock: case studies from unglaciated upland slopes in west-central Yukon; Yukon Geological Survey, Open File 2006-19, 70 p.

Bostock, H.S., 1959. Yukon Territory; *in* Tungsten deposits of Canada; Geological Survey of Canada, Economic Geology Series, no. 17, p. 14–37.

Bostock, H.S., 1970. Physiographic regions of Canada; Geological Survey of Canada, Canadian Geoscience Map 1254A, scale 1:5 000 000. https://doi.org/10.4095/108980

Bouzari, F., Hart, C.J.R., Bissig, T., and Barker, S., 2016. Hydrothermal alteration revealed by apatite luminescence and chemistry: a potential indicator mineral for exploring covered porphyry copper deposits; Economic Geology, v. 111, p. 1397–1410. https://doi.org/10.2113/econgeo.111.6.1397

Bower, B., Payne, J., DeLong, C., and Rebagliati, C.M., 1995. The oxide-gold, supergene and hypogene zones at the Casino gold-copper-molybdenum deposit, west central Yukon; *in* Porphyry deposits of the northwestern Cordillera of North America, (ed.) T.G. Schroeter; Canadian Institute of Mining, Metallurgy and Petroleum, Special Volume 46, p. 352–366.

Britten, R.M. and Marr, J.M., 1995. The Eaglehead porphyry copper prospect system, northern British Columbia; *in* Porphyry deposits of the northwestern Cordillera of North America, (ed.) T.G. Schroeter; Canadian Institute of Mining and Metallurgy, Special Volume 46, p. 530–533.

Canil, D., Grondahl, C., Laourse, T., and Pisiak, L.K., 2016. Trace elements in magnetite from porphyry Cu-Mo-Au deposits in British Columbia, Canada; Ore Geology Reviews, v. 72, p. 1116–1128. https://doi.org/10.1016/j.oregeorev.2015.10.007

CANMET, 2020. STSD-1 to STSD-4 certificate of analysis. <https://www.nrcan.gc.ca/our-natural-resources/mining-resources/certified-reference-materials/discontinued-certified-reference-materials/stsd-1-stsd-4-certificate-analysis/8023> [accessed January 24, 2020]

Casino Mining Corporation, 2014. Water quality; Chapter 7 *in* Project proposal Yukon Environmental Socio-economic Assessment Board (YESAB) submission, Volume 3. <https://casinomining.com/project/yesab-proposal/> [accessed November 5, 2019]

Casselman, S. and Brown, H., 2017. Casino porphyry copper-gold-molybdenum deposit, central Yukon (Yukon MINFILE 115J 028); *in* Yukon exploration and geology overview 2016, (ed.) K.E. MacFarlane; Yukon Geological Survey, p. 61–74.

Chapman, R.J., Grimshaw, M.R., Allan, M.M., Mortensen, J.K., Wrighton, T.M., and Casselman, S., 2014. Pathfinder signatures in placer gold derived from Au-bearing porphyries; *in* Yukon exploration and geology 2014, (ed.) K.E. MacFarlane, M.G. Nordling, and P.J. Sack; Yukon Geological Survey, p. 21–31.

Chapman, J.B., Plouffe, A., and Ferbey, T., 2015. Tourmaline: the universal indicator?; *in* Short course No. 2, Application of indicator mineral methods to exploration, 27th international applied geochemistry symposium, Tucson; Association of Applied Geochemists, p. 25–31.

Chapman, R.J., Allan, M.M., Mortensen, J.K., Wrighton, T.M., and Grimshaw, M.R., 2018. A new indicator mineral methodology based on generic Bi-Pb-Te-S mineral inclusion signature in detrital gold from porphyry and low/intermediate sulfidation epithermal environments in Yukon Territory, Canada; Mineralium Deposita, v. 53, p. 815–834. https://doi.org/10.1007/s00126-017-0782-0

Colpron, M., Nelson, J.L., and Murphy, D. C., 2006. A tectonostratigraphic framework for the pericratonic terranes of the northern Cordillera; *in* Paleozoic evolution and metallogeny of pericratonic terranes at the Ancient Pacific Margin of North America, Canadian and Alaskan Cordillera, (ed.) M. Colpron and J.L. Nelson; Geological Association of Canada, Special Paper 45, p. 1–23.

Colpron, M., Israel, S., Murphy, D., Pigage, L., and Moynihan, D., 2016. Yukon bedrock geology map; Yukon Geological Survey, Open File 2016-1, scale 1:1 000 000.

Cooke, D.R., Baker, M., Hollings, P., Sweet, G., Chang, Z., Danyushevsky, L.D., Gilbert, S., Zhou, T., White, N.C., Gemmell, J.B., and Inglis, S.I., 2014. New advances in detecting the distal geochemical footprints of porphyry systems – epidote mineral chemistry as a tool for vectoring and fertility assessments; Paper 7 *in* Building exploration capability for the 21st century; Society of Economic Geologists, Special Publication 18, p. 127–152.

Cooke, D.R., Agnew, P., Hollings, P., Baker, M., Chang, Z., Wilkinson, J.J., White, N.C., Zhang, L., Thompson, J., Gemmell, J.B., Fox, N., Chen, H., and Wilkinson, C.C., 2017. Porphyry indicator minerals (PIMS) and porphyry vectoring and fertility tools (PVFTS) – indicators of mineralization styles and recorders of hypogene geochemical dispersion haloes; *in* Proceedings of Exploration 17: Sixth Decennial International Conference on Mineral Exploration, (ed.) V. Tschirhart and M.D. Thomas; p. 457–470.

Coope, J.A., 1973. Geochemical prospecting for porphyry copper-type mineralization – a review; Journal of Geochemical Exploration, v. 2, no. 2, p. 81–102. https://doi.org/10.1016/0375-6742(73)90008-3

Day, S.J.A., Wodicka, N., and McMartin, I., 2013. Preliminary geochemical, mineralogical and indicator mineral data for stream silts, heavy mineral concentrates and waters, Lorillard River area, Nunavut (parts of NTS 56-A, -B, and -G); Geological Survey of Canada, Open File 7428, 11 p. https://doi.org/10.4095/293113

De Almeida, G.S., Marques, E.D., da Silva, F.J., Pinto, C.P., and Silva-Filho, E.V., 2019. Application of pXRF (field portable X-ray fluorescence) technique in fluvial sediments geochemical analysis – Bule Stream, Minas Gerais State, Brazil; Journal of Sedimentary Environments, v. 4, p. 143–158. https://doi.org/10.12957/jse.2019.43279

DiLabio, R.N.W., 1990. Classification and interpretation of the shapes and surface textures of gold grains from till on the Canadian Shield; *in* Current Research, Part C, Geological Survey of Canada, Paper 90-1C, p. 323–329. https://doi.org/10.4095/131269

Duk-Rodkin, A., 2001. Glacial limits, Stevenson Ridge, west of sixth meridian, Yukon Territory; Geological Survey of Canada, Open File 3804, scale l:250 000. https://doi.org/10.4095/212275

Duk-Rodkin, A., Weber, F., and Barendregt, R.W., 2002. Glacial limits map of upper Yukon River; Geological Survey of Canada, Open File 4275, scale 1:1 000 000. https://doi.org/10.4095/213393

Duk-Rodkin, A., Barendregt, R.W., Froese, D.G., Weber, F., Enkin, R., Smith, I.R., Zazula, G.D., Waters, P., and Klassen, R., 2004. Timing and extent of Plio-Pleistocene glaciations in northwestern Canada and east-central Alaska; *in* Quaternary glaciation – extent and chronology, Part II: North America, (ed.) J. Ehlers and P.L. Gibbard; Developments in Quaternary Science, v. 2, part b, p. 313–345. https://doi.org/10.1016/s1571-0866(04)80206-9

Eppinger, R.G., Fey, D.L., Giles, S.A., Kelley, K.D., and Smith, S.M., 2012. An exploration hydrogeochemical study at the giant Pebble porphyry Cu-Au-Mo deposit, Alaska, USA using high resolution ICP-MS; Geochemistry: Exploration, Environment, Analysis, v. 12, p. 211–226. https://doi.org/10.1144/1467-7873/11-RA-070

Fedortchouk, Y. and LeBarge, W., 2008. Sources of placer platinum in Yukon: provenance study from detrital minerals; Canadian Journal of Earth Sciences, v. 45, no. 8, p. 879–896. https://doi.org/10.1139/E08-032

Friske, P.W.B. and Hornbrook, E.H.W., 1991. Canada's National Geochemical Reconnaissance programme; Institution of Mining and Metallurgy, Transactions, Section B: Applied Earth Sciences, v. 100, p. B47–B56.

Garrett, R.G., Reimann, C., Hron, K., Kynčlová, P., and Filzmoser, P., 2017. Finally, a correlation coefficient that tells the geochemical truth; EXPLORE, Association of Applied Geochemists, no. 176, p. 1–10.

Garrett, R.G., 2018. The GSC applied geochemistry EDA package. <http://cran.r-project.org/web/packages/rgr/index.html> [accessed February 22, 2019]

Geological Survey of Canada, 1987. Regional stream sediment and water geochemical reconnaissance data, Yukon (NTS 115J, 115K (E1/2)); Geological Survey of Canada, Open File 1363, 142 pages (25 sheets); 1 diskette. https://doi.org/10.4095/130284

Godwin, C.I., 1975. Geology of the Casino porphyry copper-molybdenum deposit, Dawson Range, Yukon Territory; Ph.D. thesis, The University of British Columbia, Vancouver, British Columbia.

Godwin, C.I., 1976. Casino; *in* Porphyry deposits of the Canadian Cordillera, (ed.) A.S. Brown; Canadian Institute of Mining and Metallurgy, Special Volume 15, p. 344–358.

Hashmi, S, Ward, B.C., Plouffe, A., Leybourne, M.I., and Ferbey, T., 2015. Geochemical and mineralogical dispersal in till from the Mount Polley Cu-Au porphyry deposit, central British Columbia, Canada; Geochemistry: Exploration, Environment, Analysis, v. 15, no. 2, p. 234–249. https://doi.org/10.1144/geochem2014-310

Howard, H.H., McMaster, R.B., Slocum, T.A., and Kessler, F.C., 2008. Thematic cartography and geovisualization; Upper Saddle River, NJ: Pearson Prentice Hall.

Huff, L.C., 1976. A comparison of alluvial exploration techniques for porphyry copper deposits; *in* Geochemical Exploration, Proceedings of the 3rd international geochemical exploration symposium, (ed.) R.W. Boyle; Canadian Institute of Mining and Metallurgy, Special Volume 11, p. 190–194.

Huscroft, C.A., 2002a. Surficial geology, Britannia Creek, Yukon Territory (115J/15); Geological Survey of Canada, Open File 4345, 1 sheet. https://doi.org/10.4095/213868

Huscroft, C.A., 2002b. Surficial geology, Coffee Creek, Yukon Territory (115J/14); Geological Survey of Canada, Open File 4344, 1 sheet. https://doi.org/10.4095/213867

Huscroft, C.A., 2002c. Surficial geology, Cripple Creek, Yukon Territory (115J/16); Geological Survey of Canada, Open File 4346, 1 sheet, https://doi.org/10.4095/213869.

Huss, C., Drielick, T., Austin, J., Giroux, G., Casselman, S., Greenaway, G., Hester, M., and Duke, J., 2013. Casino project: Form 43-101F1 technical report, feasibility study, Yukon, Canada; Internal report, M3 Engineering and Technology Corp., 248 p. <https://www.westerncopperandgold.com/_resources/CasinoNI43-101-Jan2013.pdf> [accessed May 8, 2020].

Jackaman, W., 2011. Regional stream sediment geochemical data Stevenson Ridge, Yukon (NTS 115J & K); Yukon Geological Survey, Open File 2011-28.

Jackson, L.E. Jr., Froese, D.G., Huscroft, C.A., Nelson, F.E., Westgate, J.A., Telka, A.M., Shimamura, K., and Rotheisler, P.N., 2009. Surficial geology and Late Cenozoic history of the Stewart River and northern Stevenson Ridge map areas, west-central Yukon Territory; Geological Survey of Canada, Open File 6059, 414 p., 1 CD-ROM. https://doi.org/10.4095/248232

Kelley, K.D., Eppinger, R.G., Lang, J., Smith, S.M., and Fey, D.L., 2011. Porphyry Cu indicator minerals in glacial till samples as an exploration tool: example from the giant Pebble porphyry Cu-Au-Mo deposit, Alaska, USA; Geochemistry: Exploration, Environment, Analysis, v. 11, no. 4, p. 321–334. https://doi.org/10.1144/1467-7873/10-IM-041

Kobylinski, C.H., Hattori, K., Plouffe, A., and Smith, S.W., 2017. Epidote associated with the porphyry Cu-Mo mineralization at the Gibraltar deposit, south-central British Columbia; Geological Survey of Canada, Open File 8279, 19 p. https://doi.org/10.4095/305912

Kobylinski, C.H., Hattori, K., Smith, S.W., and Plouffe, A., 2018. High cerium anomalies in zircon from intrusions associated with porphyry copper mineralization in the Gibraltar deposit, south central British Columbia; Geological Survey of Canada, Open File 8430, 19 p. https://doi.org/10.4095/311194

Layton-Matthews, D., Hamilton, C., and McClenaghan, M.B., 2017. Modern techniques and applications to exploration; in Application of indicator mineral methods to bedrock sediments, (ed.) M.B. McClenaghan and D. Layton-Matthews; Geological Survey of Canada, Open File 8345, p. 10–24. https://doi.org/10.4095/306308

Learned, R.E., Chao, T.T., and Sanzolone, R.F., 1985. A comparative study of stream water and stream sediment as geochemical exploration media in the Rio Tanama porphyry copper district, Puerto Rico; Journal of Geochemical Exploration, v. 24, no. 2, p. 175–195. https://doi.org/10.1016/0375-6742(85)90044-5

Lehtonen, M., Lahaye, Y., O'Brien, H., Lukkari, S., Marmo, J., and Sarala, P., 2015. Novel Technologies for indicator mineral-based exploration; *in* Novel technologies for greenfield exploration, (ed.) P. Sarala; Geological Survey of Finland, Special Paper 57, p. 23–62.

Leybourne, M.I., Clark, I.D., and Goodfellow, W.D., 2006. Stable isotope geochemistry of ground and surface waters associated with undisturbed massive sulfide deposits; constraints on origin and water-rock reactions; Chemical Geology, v. 231, p. 300–325. https://doi.org/10.1016/j.chemgeo.2006.02.004

Lipovsky, P.S. and Bond, J.D., 2012. Surficial geology of Doyle Creek (115J/11), Yukon (1:50 000 scale); Yukon Geological Survey, Open File 2012-3.

Lougheed, D., McClenaghan, M.B., Layton-Matthews, D., and Leybourne, M.I., in press. Indicator minerals in till fine-fraction heavy mineral concentrates: examples from two Canadian polymetallic base metal deposits; in Targeted Geoscience Initiative 5: Volcanic- and sediment-hosted massive sulfide deposit genesis and exploration methods, (ed.) J.M. Peter and M.G. Gadd; Geological Survey of Canada, Bulletin 617.

Luck, P. and Simandl, G.J., 2014. Portable X-ray fluorescence in stream sediment chemistry and indicator mineral surveys, Lonnie carbonatite complex, British Columbia; *in* Geological Fieldwork 2013; British Columbia Ministry of Energy and Mines, British Columbia Geological Survey, Paper 2014-1, p. 169–182.

Lynch, J.J., 1990. Provisional elemental values for eight new geochemical lake sediment and stream sediment reference materials LKSD-1, LKSD-2, LKSD-3, LKSD-4, STSD-1, STDS-2, STSD-3 and STSD-4; Geostandards Newsletter, v. 14, no. 1, p. 153–167. https://doi.org/10.1111/j.1751-908X.1990.tb00070.x

Lynch, J.J., 1999. Additional provisional elemental values for LKSD-1, LKSD-2, LKSD-3, LKSD-4, STSD-1, STDS-2, STSD-3 and STSD-4; Geostandards Newsletter, v. 23, no. 2, p. 251–260. https://doi.org/10.1111/j.1751-908X.1999.tb00577.x

Mackay, D.A.R., Simandl, G.J., Ma, W., Redfearn, M., and Gravel, J., 2016. Indicator mineral-based exploration for carbonatites and related specialty metal deposits – a QEMSCAN® orientation survey, British Columbia, Canada; Journal of Geochemical Exploration, v. 165, p. 159–173. https://doi.org/10.1016/j.gexplo.2016.03.005

Mackie, R.A., Arne, D.C., and Pennimpede, C., 2017. Assessment of Yukon regional stream sediment catchment basin and geochemical data quality; Yukon Geological Survey, Open File 2017-4.

Mathur, R., Munk, L., Nguyen, M., Gregory, M., Annell, H., and Lang, J., 2013. Modern and paleofluid pathways revealed by Cu isotope compositions in surface waters and ores of the Pebble porphyry Cu-Au-Mo deposit, Alaska; Economic Geology, v. 108, no. 3, p. 529–541. https://doi.org/10.2113/econgeo.108.3.529

Mathews, W.H., 1986. Physiography of the Canadian Cordillera; Geological Survey of Canada, Map 1701A, scale 1:5 000 000.

McClenaghan, M.B. and Cabri, L.J., 2011. Gold and platinum group element indicator minerals in surficial sediments; Geochemistry: Exploration, Environment, Analysis, v. 11, no. 4, p. 251–263. https://doi.org/10.1144/1467-7873/10-IM-026

McClenaghan, M.B., and Kjarsgaard, B.A., 2007. Indicator mineral and surficial geochemical exploration methods for kimberlite in glaciated terrain: examples from Canada; *in* Mineral deposits of Canada: a synthesis of major deposit types, district metallogeny, the evolution of geological provinces, and exploration methods, (ed.) W.D. Goodfellow; Geological Association of Canada, Mineral Deposits Division, Special Publication No. 5, p. 983–1006.

McClenaghan, M.B., Parkhill, M.A., Pronk, A.G., Seaman, A.A., McCurdy, M., and Leybourne, M.I., 2017. Indicator mineral and geochemical signatures associated with the Sisson W-Mo deposit, New Brunswick, Canada; Geochemistry: Exploration, Environment, Analysis, v. 17, no. 4, p. 297–313. https://doi.org/10.1144/geochem2015-396

McClenaghan, M.B., Beckett-Brown, C.E., McCurdy, M.W., McDonald, A.M., Leybourne, M.I., Chapman, J.B., Plouffe, A., and Ferbey, T., 2018. Mineral markers of porphyry Cu mineralization: progress report on the evaluation of tourmaline as an indicator mineral; *in* Targeted Geoscience Initiative: 2017 report of activities, volume 1, (ed.) N. Rogers; Geological Survey of Canada, Open File 8358, p. 69–77. https://doi.org/10.4095/306427

McClenaghan, M.B., McCurdy, M.W., Garrett, R.G., Beckett-Brown, C.E., Leybourne, M.I., Casselman, S.G., and Pelchat, P., 2019. Mineral and geochemical signatures of porphyry copper mineralization: work in progress at the Casino Cu-Au-Mo-Ag porphyry deposit; *in* Targeted Geoscience Initiative: 2018 report of activities, (ed.) N. Rogers; Geological Survey of Canada, Open File 8549, p. 333–344. https://doi.org/10.4095/313667

McClenaghan, M.B., McCurdy, M.W., Garrett, R.G., Beckett-Brown, C.E., and Casselman, S.G., 2020. Indicator mineral signatures of the Casino porphyry Cu-Au-Mo deposit, Yukon; Geological Survey of Canada, Open File 8711, 42 p. (11 sheets). https://doi.org/10.4095/322191

McCurdy, M.W., McClenaghan, M.B., Garrett, R.G., and Pelchat, P., 2019. Geochemical signatures of the silt fraction from streams near the Casino porphyry Cu-Au-Mo deposit, Yukon Territory; Geological Survey of Canada, Open File 8632, 39 p. (41 sheets). https://doi.org/10.4095/321381

McKillop, R., Turner, D., Johnston, K., and Bond, J., 2013. Property-scale classification of surficial geology for soil geochemical sampling in the unglaciated Klondike Plateau, west-central Yukon; Yukon Geological Survey, Open File 2013-15.

Moran, K., Backman, J., Brinkhuis, H., Clemens, S.C., Cronin, T., Dickens, G.R., Eynaud, F., Gattacceca, J., Jakobsson, M., Jordan, R.W., Kaminski, M., King, J., Koc, N., Krylov, A., Martinez, N., Matthiessen, J., McInroy, D. Moore, T.C., Onodera, J., O'Regan, M., Pälike, H., Rea, B., Rio, D., Sakamoto, T., Smith, D.C., Stein, R., St John, K., Suto, I., Suzuki, N., Takahashi, K., Watanabe, M., Yamamoto, M., Farrell, J., Frank, M., Kubik, P., Jokat, W., and Kristoffersen, Y., 2006. The Cenozoic paleoenvironment of the Arctic Ocean; Nature, v. 441, p. 601–605. https://doi.org/10.1038/nature04800

Nelson, J.L., Colpron, M., Piercey, S. J., Dusel-Bacon, C., Murphy, D. C., and Roots, C. F., 2006. Paleozoic tectonic and metallogenic evolution of the pericratonic terranes in Yukon, northern British Columbia and eastern Alaska; *in* Paleozoic evolution and metallogeny of pericratonic terranes at the Ancient Pacific Margin of North America, Canadian and Alaskan Cordillera, (ed.) M. Colpron and J.L. Nelson; Geological Association of Canada, Special Paper 45, p. 323–360.

Nelson, J.L., Colpron, M., and Israel, S., 2013. The Cordillera of British Columbia, Yukon, and Alaska: tectonics and metallogeny; *in* Tectonics, metallogeny, and discovery: the North American Cordillera and similar accretionary settings, (ed.) M. Colpron, T. Bissing, B.G. Rusk, and J.F.H. Thompson; Society of Economic Geologists, Special Publication 17, p. 53–109.

Pisiak, L.K., Canil, D., Plouffe, A., Ferbey, T., and Lacourse, T., 2017. Magnetite as an indicator mineral in the exploration of porphyry deposits; a case study in till near the Mount Polley Cu-Au deposit, British Columbia, Canada; Economic Geology, v. 112, p. 919–940. https://doi.org/10.2113/econgeo.112.4.919

Plouffe, A. and Ferbey, T., 2017. Porphyry Cu indicator minerals in till: a method to discover buried mineralization; *in* Indicator minerals in till and stream sediments of the Canadian Cordillera, (ed.) T. Ferbey, A. Plouffe, and A. Hickin; Mineral Association of Canada, Topics in Mineral Sciences, Volume 47, Geological Association of Canada, Special Paper 50, p. 129–159.

Plouffe, A. and Ferbey, T., 2019. Indicator mineral content of bedrock and till at the Gibraltar porphyry Cu-Mo deposit and the Woodjam porphry Cu-Au-Mo prospect, south-central British Columbia; Geological Survey of Canada, Open File 8580, 33 p. https://doi.org/10.4095/315647

Plouffe, A., McClenaghan, M.B., Paulen, R.C., McMartin, I., Campbell, J.E., and Spirito, W.A., 2013. Processing of unconsolidated glacial sediments for the recovery of indicator minerals: protocols used at the Geological Survey of Canada; Geochemistry: Exploration, Environment, Analysis, v. 13, no. 4, p. 303–316. https://doi.org/10.1144/geochem2011-109

Plouffe, A., Ferbey, T., Hashmi, S., and Ward, B.C., 2016. Till geochemistry and mineralogy: vectoring towards Cu porphyry deposits in British Columbia, Canada; Geochemistry: Exploration, Environment, Analysis, v. 16, no. 3, p. 213–232. https://doi.org/10.1144/geochem2015-398

Plouffe, A., Kobylinksi, C.H., Hattori, K., Wolfe, L., and Ferbey, T., 2018. Mineral markers of porphyry copper mineralization: work in progress at the Gibraltar deposit, British Columbia; *in* Targeted Geoscience Initiative: 2017 report of activities, volume 1, (ed.) N. Rogers; Geological Survey of Canada, Open File 8358, p. 57–67. https://doi.org/10.4095/306423

Plouffe, A., Kjarsgaard, I., Kobylinski, C., Hattori, K., Petts, D., Venance, K., and Ferbey, T., 2019. Discovering the next generation of Cu porphyry deposits using mineral markers; *in* Targeted Geoscience Initiative: 2018 report of activities, (ed.) N. Rogers; Geological Survey of Canada, Open File 8549, p. 321–331. https://doi.org/10.4095/313666

Poulin, R.S., McDonald, A., Kontak, D.J., and McClenaghan, M.B., 2018. Assessing scheelite as an ore-deposit discriminator using its trace-element and REE chemistry; The Canadian Mineralogist, v. 56, no. 3, p. 265–302. https://doi.org/10.3749/canmin.1800005

Rebagliati, C.M., Bowen, B.K., Copeland, D.J., and Nioso, D.W.A., 1995. Kemess South and Kemess North porphyry gold-copper deposits, northern British Columbia; *in* Porphyry deposits of the northwestern Cordillera of North America, (ed.) T.G. Schroeter; The Canadian Institute of Mining and Metallurgy, Special Volume 46, p. 377–396.

Reimann, C., Filzmoser, P., Hron, K., Kynčlová, P., and Garrett, R.G., 2017. A new method for correlation analysis of compositional (environmental) data – a worked example; Science of the Total Environment, v. 607–608, p. 965–971. https://doi.org/10.1016/j.scitotenv.2017.06.063

Relf, C., 2020. Yukon Geological Survey: planning for the future; in Yukon Exploration and Geology Overview 2019, (ed.) K.E. MacFarlane; Yukon Geological Survey, p. 1–22.

Richardson, P.W., 1995. The Whipsaw porphyry system, Similkameen district, British Columbia; in Porphyry deposits of the northwestern Cordillera of North America, (ed.) T.G. Schroeter; The Canadian Institute of Mining and Metallurgy, Special Volume 46, p. 530–533.

Ryan, J.J., Zagorevski, A., Williams, S.P., Roots, C., Ciolkiewicz, W., Hayward, N., and Chapman, J.B., 2013. Geology, Stevenson Ridge (northeast part), Yukon; Geological Survey of Canada, Canadian Geoscience Map 116 (preliminary edition), scale 1:100 000. https://doi.org/10.4095/292371

Smith, C.A.S., Meikle, J.C., and Roots, C.F. (ed.), 2004. Ecoregions of the Yukon Territory: Biophysical properties of Yukon landscapes; Agriculture and Agri-Food Canada, PARC Technical Bulletin No. 04-01, Summerland, British Columbia, 313 p.

Smith, C.A.S., Sanborn, P.T., Bond, J.D., and Frank, G., 2009. Genesis of turbic cryosols on north-facing slopes in a dissected, unglaciated landscape, west-central Yukon Territory; Canadian Journal of Soil Science, v. 89, p. 611-622. https://doi.org/10.4141/CJSS09001

Taufen, P.M., 1997. Ground waters and surface waters in exploration geochemical surveys; *in* Proceedings of Exploration 97: fourth decennial international conference on mineral exploration, (ed.) A.G. Gubbins; p. 271–284.

Vavrek, M.J., Evans, D.C., Braman, D.R., Campione, N.E., and Zazula, G.D., 2012. A Paleogene flora from the upper Bonnet Plume Formation of northeast Yukon Territory, Canada; Canadian Journal of Earth Sciences, v. 49, no. 3, p. 547–558. https://doi.org/10.1139/e11-073

Wilkinson, J.J., Cooke, D.R., Baker, M.J., Chang, Z., Wilkinson, C.C., Chen, H., Fox, N., Hollings, P., White, N.C., Gemmell, J.B., Loader, M.A., Pacey, A., Sievwright, R.H., Hart, L.A., and Brugge, E.R., 2017. Porphyry indicator minerals and their mineral chemistry as vectoring and fertility tools; in Application of indicator mineral methods to bedrock and sediments, (ed.) M.B. McClenaghan and D. Layton-Matthews; Geological Survey of Canada, Open File 8345, p. 67–77. https://doi.org/10.4095/306317

Yukon Geological Survey, 2011a. Idaho occurrence (115J 099) record summary, Yukon mineral occurrence database; Government of Yukon, Yukon Geological Survey. <http://data.geology.gov.yk.ca/Occurrence/15100> [accessed January 24, 2020]

Yukon Geological Survey, 2011b. Nordex occurrence (115J 023) record summary, Yukon mineral occurrence database; Government of Yukon, Yukon Geological Survey. <http://data.geology.gov.yk.ca/Occurrence/14372> [accessed January 24, 2020].

Yukon Geological Survey, 2011c. Rude Creek occurrence (115J 022) record summary, Yukon mineral occurrence database; Government of Yukon, Yukon Geological Survey. <http://data.geology.gov.yk.ca/Occurrence/14371> [accessed January 24, 2020]

Yukon Geological Survey, 2013a. Buck occurrence (115J 071) record summary, Yukon mineral occurrence database; Government of Yukon, Yukon Geological Survey. <http://data.geology.gov.yk.ca/Occurrence/14418> [accessed January 24, 2020]

Yukon Geological Survey, 2013b. Marquerite occurrence (115J 070) record summary, Yukon mineral occurrence database; Government of Yukon, Yukon Geological Survey. <http://data.geology.gov.yk.ca/Occurrence/14417> [accessed January 24, 2020]

Yukon Geological Survey, 2015a. Mascot occurrence (115J 074) record summary, Yukon mineral occurrence database; Government of Yukon, Yukon Geological Survey. <http://data.geology.gov.yk.ca/Occurrence/14421> [accessed January 24, 2020]

Yukon Geological Survey, 2015b. Yukon digital bedrock geology. <http://www/arcgis.com/home/webmap/viewer.html?webmap=c1544758b4ff4d24ab6638e32b8465114&extent=-167.8739,55.535,-102.9666,72.0503> [accessed January 24, 2020]

Yukon Geological Survey, 2016. RGS Re-analysis. Yukon Geological Survey, point GIS layer. <http://data.geology.gov.yk.ca/Compilation/21> [accessed January 24, 2020]

Yukon Geological Survey, 2017. Zappa occurrence (115J 036) record summary, Yukon mineral occurrence database; Government of Yukon, Yukon Geological Survey. <http://data.geology.gov.yk.ca/Occurrence/14384> [accessed January 24, 2020]

Yukon Geological Survey, 2018a. Bomber occurrence (115J 027) record summary, Yukon mineral occurrence database; Government of Yukon, Yukon Geological Survey. <http://data.geology.gov.yk.ca/Occurrence/14376> [accessed January 24, 2020]

Yukon Geological Survey, 2018b. Canadian Creek occurrence (115J 101) record summary, Yukon mineral occurrence database; Government of Yukon, Yukon Geological Survey. <http://data.geology.gov.yk.ca/Occurrence/14431> [accessed January 24, 2020]

Yukon Geological Survey, 2018c. Casino occurrence (115J 028) record summary, Yukon mineral occurrence database; Government of Yukon, Yukon Geological Survey. <http://data.geology.gov.yk.ca/Occurrence/15019> [accessed January 24, 2020]

Yukon Geological Survey, 2018d. Cockfield occurrence (115J 017) record summary, Yukon mineral occurrence database; Government of Yukon, Yukon Geological Survey. <http://data.geology.gov.yk.ca/Occurrence/14367> [accessed January 24, 2020]

Yukon Geological Survey, 2018e. Zappa occurrence (115J 036) record summary, Yukon mineral occurrence database; Government of Yukon, Yukon Geological Survey. <http://data.geology.gov.yk.ca/Occurrence/14384> [accessed January 24, 2020]

Zachos, J.C., Pagani, M., Sloan, L., Thomas, E., and Billups, K., 2001. Trends, rhythms, and aberrations in global climate 65 Ma to present; Science, v. 292, p. 686–693. https://doi.org/10.1126/science.1059412